

Evolution of Venusian mantle with magmatism and compositional differentiation in a numerical modeling

Takatoshi Yanagisawa^{1*}, Masaki Ogawa²

¹IFREE, JAMSTEC, ²Graduate School of Arts & Sciences, Univ. Tokyo

The surface age of Venus is estimated to be 300-600 Myr on average, and is young in contrast to Mars, where magmatism has mostly subsided on the early stage of its history. Detailed surface observations suggest that magmatism is still ongoing on Venus, at least locally. On the other hand, Venus is a planet where the lithosphere is stagnant and plate tectonics does not operate, which is similar to Mars. When the lithosphere is stagnant, the solid-state mantle convection is unlikely to cool the mantle so efficiently as to extract all the heat internally generated by heat producing elements. In such a situation, it is crucial to take account of melting of mantle materials in the modeling of thermal history, as we suggested for the evolution of Martian mantle (Ogawa and Yanagiawa, 2011, 2012). Here, we apply our numerical model of mantle evolution with coupled magmatism for Venus to understand its thermal history, the history of magmatism, and structural evolution of the mantle. In the numerical experiments, we discuss how the crust enriched in heat producing elements develops, how the crust recycles back into the mantle, and how the mantle evolves to affect the history of magmatism and the lithosphere in accordance with the crustal evolution. We take account of the barrier effect of the phase transitions at the top of the lower mantle, and our model allows compositional differentiation of the mantle by magmatism. Based on the numerical results, we discuss the difference of evolution between Venus and Mars.

Keywords: Venus, evolution of mantle, magmatism, numerical simulation

Internal structure and thermal evolution of Mercury with highly reduced composition

Akifumi Nakayama^{1*}, Kiyoshi Kuramoto²

¹Department of Earth Sciences, School of Science, Hokkaido University, ²Department of CosmoSciences, Graduate School of Sciences, Hokkaido University

According to topography, surface composition and gravity data obtained by MESSENGER, a new internal structure model of Mercury have been proposed (Smith et al., 2012). The core radius and solid mantle density have been estimated on the basis of the moment of inertia are 2030 +/- 37 km and 3650 +/- 225 kg m⁻³, respectively. To explain the high mantle density, the presence of FeS layer at the bottom of mantle is suggested. The observed surface composition (Nittler et al., 2011) is poor in FeO. This suggests Mercury formed from highly reduced precursors like enstatite (E) chondrite (Wasson, 1998). Because these results are very different from the previous model, it is necessary to reestimate the precursors and thermal evolution of Mercury.

E chondrite contains significant amount of S in metal components. If such a significant amount of light element is also contained in the Mercurian core, silicate mantle layer should be very thin in order to explain the higher average density of Mercury. In previous thermal evolution models assumed the relatively thick silicate mantle (e.g. Stevenson et al., 1983), the fluid core is not thermally convective today, because heat transport through the mantle sufficiently decreases. If this is the case, no FeS is solidified in the core. However if Mercury has a thin mantle, the heat transport efficiency through the mantle does not decrease so much and the core could be cooled to allow FeS solidification. In this study we calculate the thermal evolution of Mercury with supposing new internal structure and discuss thermal state of the core and thermal history of Mercury.

Assuming spherical symmetry, the heat balance calculation of silicate mantle and core performed in accordance with the mixing length theory (Abe, 1997) and box model (Stevenson et al., 1983), respectively. The silicate and metal components have chemical compositions similar to those of E chondrite, respectively. The thickness of silicate mantle and the core density are 170-340 km and 6000-6981 kg m⁻³, respectively, which agree with the core radius and solid mantle density estimated by Smith et al. (2012). In this calculation we varied the mantle thickness while adjusted the concentration of sulfur in the core, so as to keep the mean density of Mercury. The viscosity of a silicate mantle assuming enstatite composition is about 1000 times that of the Earth's upper mantle, hence the heat transport efficiency by convection is weaker than previous models. We give the solidus temperature of enstatite for the initial temperature of mantle, and the adiabatic temperature distribution continuous with the temperature of the core-mantle boundary (CMB) for the initial temperature of the core. Initial temperature of the core is higher than the melting curve of Fe-S alloy, so the core is entirely molten.

In all the models of different mantle thickness, heat transport by convection is weakened rapidly and dominant heat transport mechanism is switched to thermal conduction during the first 1 billion year. Heat is still efficiently transported by thermal conduction, because the silicate mantle is thinner than previous models. When the silicate mantle is thinner than 270 km, the temperature of the CMB drops below the eutectic point of Fe-FeS binary within 4.5 billion years. This explains the formation of solid FeS layer. In addition, the heat flow across CMB after 4.5 billion years exceeds the value achieved by the thermal conduction in the core with adiabatic temperature profile. This suggests that it is possible to drive the liquid outer core dynamo by the thermal convection even today.

Keywords: Mercury, thermal evolution

Mantle convection in super-Earths with high compressibility, high Rayleigh number, and temperature-dependent viscosity

Takehiro Miyagoshi^{1*}, Chihiro Tachinami², Masanori Kameyama³, Masaki Ogawa⁴

¹IFREE/Jamstec, ²Department of Earth and Planetary Sciences, Tokyo Institute of Technology, ³Geodynamics Research Center, Ehime University, ⁴Department of Earth Sciences and Astronomy, University of Tokyo

Understanding mantle convection in super-Earths is a key to clarifying their habitability, because mantle convection determines the surface environment and the magnetic field intensity through the influence on the activity of core convection. The large size of super-Earths implies that the depth of their mantle far exceeds the thermal scale height. In this paper, we present numerical simulation results of mantle convection in super-Earths with high compressibility, high Rayleigh number, strongly temperature-dependent viscosity and depth-dependent thermal expansivity.

Thermal convection of compressible infinite Prandtl number fluid is solved in a rectangular box under anelastic approximation by the ACuTEMAN (Kameyama et al. 2005). The model of the super-Earths, including depth-dependent thermal expansivity and density, is the same as Tachinami et al. (2013, submitted). The dissipation number is 5, which corresponds to terrestrial planets of ten times the Earth's mass. The Rayleigh number defined with the viscosity at the core-mantle boundary (CMB) Ra is from $6E6$ to $1E10$. A viscosity contrast r up to $1E7$ arises between the CMB and the surface owing to the temperature-dependence of viscosity. The employed grid number is 1024 (horizontal) and 256 (vertical).

Numerical results show that the efficiency of heat transport by the mantle convection in super-Earths becomes smaller than that in the Earth owing to adiabatic compression effect. For example, at $Ra=1E10$ and $r=1E3$, the Nusselt number is only about twenty, less than the expected value when the effect of adiabatic compression is neglected. This low efficiency of heat transfer strongly affects the evolution of the super-Earths. The magnetic field of super-Earths, for example, is probably weak because the core is not cooled efficiently. The weak magnetic field can be fatal for the habitability of super-Earths. We also found that in some cases it takes time longer than the age of the Universe for the calculated mantle convection to go through with the initial transient stage. This suggests that the initial transition stage, not the statistically steady stage, is more relevant to most of the time in the evolutionary history of super-Earths. The temperature and flow field show that at high Ra and at strong temperature-dependent viscosity the stratosphere develops in the middle of the mantle. Hot plumes from the CMB does not ascend to the surface of the planet. Cold plumes that grow at the base of the lithosphere are weak or are totally inhibited by the strong effect of adiabatic compression. The thermal structure of the mantle in super-Earths is totally different from that of the Earth.

Keywords: mantle convection, super-Earths

Laboratory generation and observation of super-Earth's interior using high-power laser

Norimasa Ozaki^{1*}, Tomoaki Kimura³, Takuo Okuchi⁴, Martin French⁵, Tomoyuki Kakeshita¹, Mika Kita¹, Kohei Miyanishi¹, Ronald Redmer⁵, Takayoshi Sano⁶, Tomokazu Sano¹, Katsuya Shimizu⁷, Tomoyuki Terai¹, Ryosuke Kodama¹

¹Graduate School of Engineering, Osaka University, ²Photon Pioneers Center, Osaka University, ³Geodynamics Research Center, Ehime University, ⁴Institute for Study of The Earth's Interior, Okayama University, ⁵Institut für Physik, Universität Rostock, ⁶Institute of Laser Engineering, Osaka University, ⁷Center for Quantum Science and Technology under Extreme Conditions, Osaka University

We reports the first laboratory generation of super Earth planet interior states. We focused a high-power laser pulse onto a water target, thereby dynamically compressing the water to pressures to ~100-200 GPa. Our pressure-volume-temperature equation-of-state data are in good agreement with water-world super Earth GJ1214b interior conditions predicted by first principle calculations. Simultaneous optical reflectivity measurements also show that the warm dense water behave as an electronically conducting fluid capable of generating a significant magnetic field. This high-power laser experiment is an important step toward understanding the interior structure of super Earths, which can provide a clue for understanding a scenario for formation of the exoplanetary systems.

Keywords: Super Earth, Water, High pressure, Phase transition, Power laser, Laser shock

Anelastic convection model in rotating spherical shells for stars, gas and icy giant planets.

Youhei SASAKI^{1*}, Shin-ichi Takehiro², Kensuke Nakajima³, Yoshi-Yuki Hayashi⁴

¹Department of Mathematics, Kyoto University, ²Research Institute for Mathematical Sciences, Kyoto University, ³Department of Earth Planetary Sciences, Kyushu University, ⁴Center for Planetary Science/Department of Earth and Planetary Science, Kobe University

The problem of convection in rotating spherical shells has been studied vigorously as a fundamental model of global convection presumably emerging in celestial bodies, such as stars, gas and icy giant planets, and terrestrial planetary interiors. Recently, according to development of numerical computational abilities, fundamental aspects and characteristics of convection have been revealed and knowledge about this issue is increased under the assumption of Boussinesq approximation, which ignores compressibility of the fluid. However, compressible convection in rotating spherical shells has not yet understood compared with Boussinesq convection, although some studies performed so far use the anelastic approximation in order to deal with compressibility. Compressibility is an important element for discussing deep convection of stars, gas and icy planets, since thickness of their convection layers is several times larger than the scale height. Not only for these celestial bodies but also for extra-solar gas giant planets, which have been so many discovered with recent sophisticated technologies of astronomical observations, compressibility could not be ignored for considering fluid motion in their interiors. Investigation into effects of compressibility on convection in rotating spherical shells is expected to contribute to the basic knowledge for considering fluid motions in the interiors of these many celestial bodies.

In the present study, we develop a numerical model of an anelastic fluid in rotating spherical shells in order to assess effects of compressibility on convective motions. The governing equations are anelastic equations with polytrope basic state. We already developed numerical model of Boussinesq convection in rotating spherical shells as a member of Hierarchical Spectral Models for Geophysical Fluid Dynamics "SPMODEL". On the development of the anelastic model, we extended our numerical model of Boussinesq convection in rotating spherical shells accomplished so far to the anelastic system.

In all calculations, the ratio of inner and outer radii, the Prandtl number, the Ekman number are fixed to 0.35, 1, 10^{-3} , respectively. The Rayleigh number is also fixed 1.2 times the critical Rayleigh number. The inverse density scale height, N , is varied from 10^{-5} , 1, 2, 3, and 5. For each combination of parameters, time integration is carried out until quasi-steady state is established. When the case of N is 10^{-5} , columnar convection along the rotation axis emerged near the inner boundary. This feature is similar the Boussinesq case. On the other hand, the location of convection column becomes close to the outer boundary, and the convective motion occurs are near the outer boundary as the value of N is increased.

Keywords: Convection in rotating spherical shells, Compressible convection, Anelastic equation

Ancient Cratered Southern Highland Province, Mars:

James Dohm^{1*}, Shigenori Maruyama¹, Hideaki Miyamoto²

¹Earth-Life Science Institute, Tokyo Institute of Technology, ²The University Museum, The University of Tokyo

The geologic provinces of Mars, as identified through a synthesis of geologic, paleohydrologic, topographic, geophysical, spectral, and elemental information [1], are windows into its evolution, with the ancient southern highland province being a key to the extremely ancient geological and possible biological pasts. The ancient cratered southern highland province includes Noachian (>3.7Ga) geologic terrains that are marked by magnetic anomalies [1]. The terrains include: (1) Noachian mountain ranges, Thaumasia highlands and Coprates rise, both of which exhibit complex structures such as thrust and normal faults and rift systems, as well as cuestas and hogbacks along their margins, (2) basin and range topography, including salt-containing, structurally-controlled basins, as exemplified at Terra Sirenum, (3) faults that are tens to thousands of kilo-meters long, and (4) degraded promontories, many of which are interpreted as silica-rich volcanoes or in some cases, impact crater massifs.

These terrains can be aptly explained through dynamic endogenic activity, including some form of primitive plate tectonism and/or mobile crust, as well as planetary shrinkage due to cooling, rather than impact events. The ancient cratered southern highland province could comprise extremely ancient (>3.9 Ga) geologic and habitable environmental information, including granite and primordial continental crustal materials. Such materials are considered to be critical to the emergence to life on Earth [2].

References

- [1] Dohm, J.M. et al., (2013?in press), Mars evolution. Nova Science Publishers, Inc.
- [2] Shigenori Maruyama, this conference.

Control mechanisms of the tropopause level and cloud top in Jovian atmosphere.

Yasuto TAKAHASHI^{1*}, George HASHIMOTO², Masanori Onishi³, Kiyoshi Kuramoto¹

¹Hokkaido Univ, ²Okayama Univ, ³Kobe Univ

The primary definition of the tropopause of a planetary atmosphere may be the level which divides the convective region and upper stably stratified region. On the other hand, the tropopause is often defined as the level of first temperature minimum which occurs in the temporal-mean vertical temperature profile above the surface. This definition makes it easy to find the tropopause altitude, but it may be an approximation of the true boundary between the two regions, because the stably stratified region possibly includes a layer with negative vertical temperature gradient. This approximation could work for the Earth atmosphere because the change in lapse rate around the tropopause level is sharp and therefore the difference from the primary definition is minimal, but being not sure whether it is applicable for another planet or not.

Equilibrium cloud condensation models (ECCMs, e.g. Weidenschilling and Lewies 1973) and cloud convection models (e.g. Sugiyama et al. 2011) assume that the Jovian atmosphere is enough convective in the region below a level about 0.1 bar, where the temperature minimum exists in the representative temperature profile retrieved by observations. However, we need to revisit it more carefully as mentioned above. In a radiative-convective model of Jovian atmosphere (Appleby and Hogan, 1984), the temperature minimum occurs at a level around 0.1 bar, while the radiative-convective boundary may occur at a much deeper level around 0.5-0.75 bar. It means that the generation of NH₃ cloud by convection, a widely accepted picture for the Jovian uppermost cloud formation, may be indeed marginally possible because little NH₃ would condense at such deeper level.

In order to understand how the tropopause level is controlled in the Jovian atmosphere, we utilizes a new numerical model of radiative-convective equilibrium in H₂-rich atmosphere taking into account the up-to-dated gas absorption models and knowledge on the atmospheric composition. Our model is a 1D radiative-convective equilibrium model for a plane parallel atmosphere. In this model, the temperature of lower boundary (taken 10 bar) is given constant in accordance with the Galileo probe data. We only solve the transfer of long wave radiation with wave number range from 0 to 10,000 cm⁻¹. Here, we use HITRAN2008 database (Rothman et al. 2009) for line absorption for condensable gas species, and Borysow (1989, 2002) for continuum absorption due to H₂-H₂ and H₂-He collision. The temperature of each atmospheric layer is changed step by step according to the calculated amount of radiative heating or cooling until it converges into the steady state, or radiative-convective equilibrium state with applying convective adjustment for the unstable layer. Atmospheric compositions are given within the range consistent with the Galileo probe experiment.

From our preliminary results, it is confirmed that the tropopause by primary definition is formed around 0.5 bar level almost independent on the mixing ratio of condensable species. Note that the temperature tends monotonically decreases with altitude for most cases because the solar heating is neglected in these calculations. If the solar heating was included, the tropopause level would likely shift deeper. Our obtained temperature profiles are compared with the NH₃ condensation curves, showing that little NH₃ condensation occurs within the convective region when given nominal NH₃ concentration or below. On the other hand, a NH₃ condensable layer spans above the tropopause. This implies that the uppermost cloud layer of Jovian atmosphere would be mostly composed of stratospheric cloud and/or convective cloud associated with upwelling penetrating stratosphere. Because the uppermost cloud play an important role in determining the planetary albedo, model development for cloud formation in the stratosphere would be essential to understand the radiative energy budget in the Jovian atmosphere.

Keywords: Jupiter, Atmosphere, Cloud, Tropopause, Radiative transfer

Follow-up Observation of Jupiter's Atmosphere 19 Years after the SL9 Event

Takahiro IINO^{1*}, Tac Nakajima¹, Tomoo NAGAHAMA¹, Akira Mizuno¹

¹Solar-terrestrial Environment Laboratory, Nagoya University

Cometary Impact as the Supply Source of Volatile Gases on Planetary Atmosphere

In 1994, the impact of comet Shoemaker-Levy 9 (hereafter SL9) had changed the Jupiter's atmospheric composition. The abundance of CO and HCN had increased vigorously to realize 10^3 to 10^4 times larger value than before the SL9 event. Besides, some S-bearing molecules were found and produced newly (Moreno et al. 2003). Similarly, on Neptune, it is expected that similar impact process has realized 50 ? 1000 times as large CO abundance as the other three gas giants (Lellouch et al. 2005) (A. Marten et al. 2005). Studies on such huge disturbance induced by cometary impact is very important because such process can affect the atmospheric composition of gas giant largely. Revealing the chemical evolution of the solar system planet's atmosphere is main issues in planetary science. Detailed studies on the entire chemical processes from cometary impact to the end of reaction are needed.

Our observation in 2012

Studies on the SL9 event and its aftermath are very important especially because it is the only case where the cometary impact can be monitored in detail. Even now, little is known about how long the influence of the SL9 continues to affect on Jupiter's atmosphere. Constructing and examining the chemical evolution are the key for full understanding of cometary impact as part of atmospheric evolution processes.

We have focused on the sulfur chemistry because CS and S-bearing species were known to be produced after the SL9 event. Studies on the chemical evolution of S-bearing species suggest that CS is a daughter species of S₂ and CS₂, and had been continuously produced for a year after the SL9 event (Moses et al. 1995). This scenario is supported by stable abundance variations measured from 1995 to 1998 (Moreno et al. 2003). However, since no observation was reported since 2003, we have planned a new observation of impact remnant gases to obtain their abundance and derive their decay time in 2012. We observed CS(J=2-1), CO(J=1-0) and HCN(J=1-0) rotational lines in millimeter waveband using Nobeyama 45-m telescope of NAOJ. Our observation found that CS abundance has decreased significantly, placing its upper limit as one tenth of the abundance measured in 1995. The finding may allude to a hypothetical scenario that the CS destruction process has already begun and its destruction mechanism may be due to photochemical evolution.

CS Destruction Processes and Our New Observation Plans

It is suggested that only a few processes can remove CS permanently (Moses et al., 1996). Furthermore, photo-dissociation process is important as well because the lifetime of CS against photolysis is very short at 1AU (Canaves et al., 2001) and as to be taken into account. We have tested the recycling process of photolysis with simple one-box model. The modeled time variation of the CS abundance, assuming the lifetime of CS only, as against photolysis has shown clear discrepancy with the observed result. Thus, dissociated S atom is suggested to be recycled.

We are planning new observation to obtain CS abundance with more sensitive observation in sub-millimeter waveband. Next, survey observation of S-bearing species which are candidates of daughter species of CS. In this presentation, detail of our observation and a model of chemical processes will be presented.

Moreno, R, A. Marten, H.E Matthews, and Y Biraud. 2003. *Planetary and Space Science*, 51, 591-611

Lellouch, E, R Moreno, and G Paubert. 2005. *A&A*, 40, 37-40.

Marten, A, H E Matthews, T Owen, R Moreno, T Hidayat, and Y Biraud. 2005. 1097-1105.

Moses, J. I. 1996. *The Collision of Comet Shoemaker-Levy 9 and Jupiter: IAU Colloquium 156*, 243 - 268

Moses, J. I, A, Allen. 1995. *GRL*, 22, 1597-1600

Canaves, M. V., A. A. de Almeida, D.C. Boice, G. C. Sanzovo. 2007. *Adv. In Space Res.* 39, 451-457

Keywords: Jupiter, comet, radio astronomy

Hugoniot curve for forsterite under extreme conditions: O₂ supply into the surface environment on the early Earth

Kosuke Kurosawa^{1*}, Toshihiko Kadono², Yoichiro Hironaka³, Keisuke Shigemori³, Hideharu Kuwahara⁴, Tatsuhiro Sakaiya⁵, Takayoshi Sano³, Sohsuke Ohno⁶, Toshimori Sekine⁷, Norimasa Ozaki⁸, Ryosuke Kodama⁸, Shogo Tachibana⁹, Takafumi Matsui⁶, Seiji Sugita⁴

¹Institute of Space and Astronautical Science, Japan Aerospace Exploration Agency, ²School of Medicine, University of Occupational and Environmental Health, ³Institute of Laser Engineering, Osaka University, ⁴Department of Complexity Science and Engineering, The University of Tokyo, ⁵Department of Earth and Space Science, Osaka University, ⁶Planetary Exploration Research Center, Chiba Institute of Technology, ⁷Department of Earth and Planetary Systems Science, Hiroshima University, ⁸Division of Electrical, Electronic and Information Engineering, Osaka University, ⁹Earth and Planetary System Science Department of Natural History Sciences, Hokkaido University

Recent dynamical model for impact flux to the Earth-Moon system based upon the chemical analyses of lunar samples and crater chronology suggests that impactors during the late heavy bombardment period are highly dynamically excited and their impact velocities to the Earth reach ~ 30 km/s. The amount of silicate vapor and its chemical composition, which are important factors to investigate the geological consequence after such hypervelocity impacts, have not been understood. This is because reliable Hugoniot curve for silicate materials higher than 200 GPa is not established due to technical difficulties, resulting in large uncertainty in the thermodynamic path of isentropic release from shocked state. Although there is an EOS model, M-ANEOS, for silicate materials which is widely used for hydrocode calculations [e.g., Canup, 2012, Cuk & Stewart, 2012], the entropy gain for silica predicted by M-ANEOS is considerably smaller than that investigated by experiments. In this study, We carried out laser shock experiments at GEKKO XII-HIPER facility of Institute of Laser Engineering of Osaka University to obtain the Hugoniot curve for actual silicate material, forsterite, up to 1200 GPa on an entropy-pressure (S-P) plane. Shock temperatures and pressures during the propagation of laser-induced shock waves were measured simultaneously. Shock-induced entropy gain can be calculated using the obtained peak shock temperatures and pressures and thermodynamic relations. We found that the entropy gain for forsterite is much larger than the M-ANEOS prediction as well as silica. The amount of forsterite vapor after isentropic release can be calculated using the lever rule when the shock-heated forsterite is under thermal equilibrium during expansion. The amount of forsterite vapor is ~ 2 times than the M-ANEOS prediction. The redox state in impact-induced vapor clouds strongly depends on the degree of vaporization of silicates because the molar fraction of oxygen in silicate materials is higher than 0.5. Then, we conducted thermochemical calculation along with the isoentropes at ~ 30 km/s to calculate the molecular composition of released gas into the atmosphere after a meteoritic impact with CI-like chemical composition. We found that a large amount of molecular oxygen, which is not considered to be existed on prebiotic Earth, is likely to be released into the atmosphere. Hypervelocity impacts during the late heavy bombardment period might supply a large amount of oxygen into the surface environment. Such impact-induced oxygen might play important roles in a chemical evolution phase on the early Earth because oxidation reaction by molecular oxygen produced a large amount of free energy.

Keywords: Meteoritic impacts, Forsterite, Late heavy bombardment, Laser shock compression, Hugoniot curve, Surface environment on the early Earth

Revised fragmentation model of planet-sized collisions

Tomoaki Fujita^{1*}, Hidenori Genda¹, Hiroshi Kobayashi², Hidekazu Tanaka³, Yutaka Abe¹

¹Department of Earth and Planetary Science, Graduate School of Science, The University of Tokyo, ²Department of Physics, Nagoya University, ³Institute of Low Temperature Science, Hokkaido University

In the process of planet formation, collisions between planetesimals or a planetesimal and a protoplanet occur frequently and let them grow up. Recent studies (e.g., Kobayashi and Tanaka 2009) suggest that the upper limit on the mass of planets varies by the amount or size of fragments scattered by such collisions. Therefore, in order to develop the more accurate theory of planet formation, it is important to investigate how destructive each collision is under various conditions. The critical impact energy for catastrophic disruption Q_D^* , where the largest remnant has half the target mass, has been well investigated under various conditions (e.g., Benz and Asphaug 1999), and only this value has been regarded as important for the planet formation to date. However, there are some doubtful points in the accuracy of this value because of the low-resolution simulations and unclearness of the analytical method. Moreover, according to Kobayashi and Tanaka 2009, the collisions with less than critical impact energy are also important for planet formation. Although they presumed that the total mass of fragments is linear with the impact energy, its dependence on impact energy has not been examined.

We systematically performed the hydrodynamic simulations of collisions with various impact energies in SPH method, and reexamined Q_D^* and investigated a relation between total mass of ejected material and impact energy. In our simulations, bodies with different size collide against 100km- and 10km-diameter bodies at different speed, and the amount of the total mass of ejected material can be calculated. In addition, we checked the dependence on the resolution and performed simulations in high enough resolution, and analyzed with the original analytical method, that can be recognized objectively.

We found that the Q_D^* value we derived is about one order of magnitude smaller than that of the previous work (Benz and Asphaug 1999). This means collisions between planetesimals or a planetesimal and a protoplanet are more destructive than before.

In the case of collisions with impact energy less than Q_D^* , contrary to the expectation of Kobayashi and Tanaka 2009, the total mass of fragments is not linear with the impact energy due to the curvature of the target. On the other hand, in the case of collisions with very low impact energy, the effect of the curvature is so slight that the total mass of fragments is linear with the impact energy. Considering these two facts, the fragmentation model can be built on such a small scale.

Moreover, since we improved the existing SPH code, it became possible to evaluate the collisions where the not gravity but material strength is dominant; the size of target is less than 1km-diameter. Then, we are going to show this result.

Keywords: planet formation, fragmentation, planetesimals

Analysis of shocked quartz grains inside the Chicxulub crater and constraints on ejecta deposition processes.

Yu Chang^{1*}, Kazuhisa Goto², Yasuhito Sekine³, Eiichi Tajika³

¹Earth and Planetary Sci., Univ. of Tokyo, ²Tohoku Univ. IRIDeS, ³Complexity Sci. & Eng., Univ. of Tokyo

Impact cratering is a ubiquitous process which occurs on terrestrial planets and small bodies in the solar system. Geological and geochemical studies of impact craters on Earth provide essential and unique information, such as a three-dimensional structure and lithological characteristics of craters, for understanding impact cratering process. The Chicxulub crater, located in the Yucatan Peninsula in Mexico, is 180-200 km in diameter, which is one of the largest impact structures found on Earth. This impact event is considered to have caused a mass extinction at the Cretaceous-Paleogene (K-Pg) boundary at 66 Ma. Thus, knowledge on the cratering process associated with the Chicxulub impact event will be important both for understanding the cratering process of a large-scale impact and its environmental consequences. However, the detailed formation processes of the Chicxulub crater have been still unknown.

In this study, we analyzed both the size distribution of and planar deformation features (PDFs) on shocked quartz grains contained in the Yaxcopoil-1 (YAX-1) drilling core samples derived from the Chicxulub crater. PDFs are planar micro structures generated under high-pressure conditions (~10-35 GPa). The crystallographic orientation of PDFs is known to preserve information of shock pressure achieved by impacts. We found 525 shocked quartz grains from top to bottom of impactite sequences in the YAX-1 core. In the present study, 574 sets of PDFs were measured from fifteen vertical levels in the impactite sequences.

We found that shocked quartz grains in the impact melt layer (Unit 5) of the YAX-1 core were predominantly undergone high shock pressures (>25 GPa). Whereas, shocked quartz found in other impactite sequences (i.e., Units 6 and 4-1, in ascending stratigraphic order) are mixtures of quartz grains experienced various shock pressures. These results suggest that Unit 5 is likely to have been formed by an outward flow of impact melt-sheet from the transient crater cavity during the central uplift and collapse of the transient crater. In Unit 1, i.e., the uppermost impactite units, we found an opposite correlation between shocked quartz grains undergone high peak shock pressures (>25 GPa) and those undergone medium degree of shock pressures (12-25 GPa) associated with upward grain fining in the sequences. These results strongly support the idea that Unit 1 was repeated impact-induced tsunami deposits. Given both our results of impact melt-sheet origin of Unit 5 and the results of hydrodynamic simulation of the Chicxulub crater, Unit 6, underlying Unit 5, could be interpreted as ejecta curtain deposits. Our results of ejecta curtain deposits of Unit 6 provide the geological evidence that the position of YAX-1 core is located outside the transient crater cavity, which support the hydrodynamic simulations and seismic data of the Chicxulub crater.

Keywords: impact cratering, Chicxulub crater, shocked quartz, Planar deformation features (PDFs)

Impact crater formation on the snow-ice layered structure

Masahiko Arakawa^{1*}, Mika Saita¹, Minami Yasui²

¹Graduate School of Science, Kobe University, ²Organization of Advanced Science and Technology, Kobe University

Impact craters are found on every solid bodies in the solar system, and they are formed by high speed impacts of small bodies. The study on the crater scaling law has been conducted to estimate the formation condition of these craters, so the cratering experiments have been made for the various materials to refine the scaling law. The icy bodies which exist usually in the outer solar system have a wide variety of the size and the density, and the icy bodies with the middle and the large sizes could be covered with the snow regolith on the icy crust. In this two layer structure, the crater size and the formation condition of the crater on the icy crust could be affected by the regolith layer. However, there are no cratering experiments on two layer structure made of snow and ice although most of the experiments were made for the homogeneous rock and ice or the basalt block covered with rocky regolith. In this study, we tried to clarify the effect of the snow regolith layer on the crater formed on the ice layer. Moreover, the particle velocity of snow layer should be determined to estimate the crater size formed on the ice block. Then, the snow plate simulating the regolith layer was used to measure the particle velocity and it was used to refine the scaling law applicable to the layered structure on the icy bodies.

Impact experiments were made by using a vertical gas gun set in a cold room at -10 degree. The cylindrical projectile was launched at 300 and 450m/s and made of ice and polycarbonate. The mass of ice and polycarbonate is 1.60g and 1.68g, respectively. The ice target was a rectangular ice block with the mass of 8kg. The ice block was covered with a snow layer which was made of ice particles with the size less than 710 microns and the snow thickness was from 5 to 30mm. After the impact, the crater formed on the ice block was measured to describe the diameter, the volume and the depth. In the case of the measurements of particle velocity for snow plates, the snow plate thickness was changed from 10 to 40mm and they were impacted by an ice and a polycarbonate projectile. A high speed digital video camera was used to record the ejection of the snow particles with the frame rate of 2×10^4 to 5×10^3 .

We found that the antipodal velocity of the snow plate decreased with the increase of the plate thickness at the constant impact velocity. Moreover, the decay rate of the particle velocity for ice projectile was found to be larger than that for polycarbonate projectile. The ice projectile was completely disrupted at the moment of impact but the polycarbonate projectile was observed to be intact through the snow plate, so that it was recovered without disruption. The relationship between the antipodal velocity of v_e and the plate thickness (t) was obtained to be $v_e = a t/d^{-b}$, where d is the thickness of the projectile 10mm.

In the case of the cratering experiments, we compared the crater size formed on the ice block for ice projectile with that for polycarbonate projectile and noticed that the crater formed by ice projectile was always smaller than that formed by the polycarbonate projectile at the constant impact velocity. The crater size decreases with the increase of the thickness of the snow plate for each projectile and each relationship was empirically determined. This relationship was theoretically related to the particle velocity of snow plate at the boundary between snow plate and ice block. This theory was proposed in Dohi et al. (2012), in which the crater scaling law was extended to the two layer target. We applied their modified scaling parameter Pi^* to our results and obtained the following relationship between the crater volume and the Pi^* , $Pi_v = 2.05 \times 10^{-9} Pi^*{}^{-2.6}$.

Dohi, K., Arakawa, M., Okamoto, C., Hasegawa, S. and Yasui, M. (2012) The effect of a thin weak layer covering a basalt block on the impact cratering process, *Icarus*, 218, 751-759.

Keywords: regolith, icy bodies, crater, layered structure, scaling law, shock wave

PERC CubeSat project: Meteor-observing satellite S-CUBE (S3)

Ryo Ishimaru^{1*}, SAKAMOTO, Yuji², KOBAYASHI, Masanori¹, NAMIKI, Noriyuki¹, SENSU, Hiroki¹, WADA, Koji¹, OHNO, Sohsuke¹, ISHIBASHI, Ko¹, YAMADA, Manabu¹, ARAI, Tomoko¹, MATSUI, Takafumi¹, HOSOKAWA, Shigeru¹, TANABE, Yuta², YAGISAWA, Hitoshi², ABE, Shinsuke³, KUROSAWA, Kosuke⁴, NAKASUKA, Shinichi⁵, YOSHIDA, Kazuya², AKIYAMA, Hiroaki⁶, SATO, Mitsuteru⁷, TAKAHASHI, Yukihiro⁷

¹Planetary Exploration Research Center, Chiba Institute of Technology, ²Tohoku University, ³Institute of Astronomy, National Central University, ⁴JAXA, ⁵The University of Tokyo, ⁶Wakayama University, ⁷Hokkaido University

Introduction: A CubeSat is a type of miniaturized satellite for space research. The standard 10*10*10 cm cubic satellite is often called a 1U CubeSat meaning one unit, and has a mass of 1 kilogram. CubeSat has been a familiar tool for engineers to test new technologies in space and often used for Earth remote-sensing, too. On the other hand, use of CubeSat for astronomical and planetary sciences has been rare because of severe constraints on payload. We propose in this work to use a CubeSat for the first time in planetary sciences, specifically to observe meteors entering into Earth's atmosphere. A development of a science-oriented CubeSat brings about many difficulties, but our challenge can possibly open a new field of observational research in astronomy and planetary sciences. An advantage to use a CubeSat in comparison with previous missions led by national space agency is that a CubeSat project can be carried out within a limit of cost, technology, and organization available in academy. This allows a development of a satellite in a few years.

Our new project is called "Shooting star Sensing Satellite (S3: S-CUBE) Project." The S-CUBE Project was a project started by a partnership between Planetary Exploration Research Center of Chiba Institute of Technology (PERC/Chitech) and Tohoku University to develop a 3U CubeSat (30*10*10 cm; 4 kg) based on the design of RAIKO that was developed and launched by Tohoku University in October, 2012. The S-CUBE is equipped with optical sensors, such as a camera and photomultipliers, to observe luminous emission of meteors from a low-Earth orbit. The launch date is planned in the 2014. For command uplink and data downlink, an UHF antenna and an S-band antenna at Chitech are used.

Scientific Objectives: Meteors are luminous phenomena induced by hypervelocity entry of meteoroids into the Earth's atmosphere. Because most meteoroids are thought to be originated from comets and asteroids, the meteor give us valuable opportunities of an indirect exploration of the primordial objects in the solar system.

Although meteors have been observed mainly from the ground so far, the ground-based observations have weak points: narrow observational range and weather dependent. In contrast to the ground-based observations, a space-based observation by an earth-orbiting satellite enables a continuous global observation of meteors. Further, a space-based observation can detect ultraviolet emission from meteors because it is not hindered by ozone layer.

The S-CUBE is designed to be equipped with one camera and 2 (or possibly 4) photo multiplier. The camera points nadir direction to take images of meteors during flight over the night side of the Earth. We can estimate the meteoroid size from brightness of meteors. The photo-multipliers are attached with UV band-pass filters so as to extract UV light of meteors from lights from the Earth. Detection of UV light of meteors is used as a trigger of the camera. It is also suggested that UV light of meteors includes emissions of some light elements, such as sulfur, which have not been observed by previous ground-based observations.

Keywords: Meteor, CubeSat, Optical observation, UV observation

3D FDTD simulation of Rosetta/CONSERT radar tomography observation

Takao Kobayashi^{1*}

¹Korea Institute of Geoscience and Mineral Resources

Rosetta is a comet exploration project of ESA which aims to approach Comet 67P/Churyumov-Gerasimenko in 2014. It carries various onboard missions, one of which is a radar tomography mission called Comet Nucleus Sounding Experiment by Radiowave Transmission (CONSERT). CONSERT consists of two radar systems on the Rosetta platform and on the Philae lander, and is to perform bi-static radar sounding observations by using CONSERT transmits radar pulses of which the center frequency is 90 MHz.

We built a 3D simulation code based on Finite Difference Time Domain (FD-TD) algorithm. It simulates CONSERT observation in which the Philae lander transmits radar pulses and the Rosetta platform received them. The Philae radar transmitter is approximated by a point current source whose pulse shape is a differentiated Gaussian. Received echo at the Rosetta platform was approximated by the electric field at the receiving point, which was calculated by based on Near-to-Far-Field conversion algorithm. The comet nucleus model is represented by spatial distribution of dielectric constant in the simulation space.

The simulation results are utilized in developing the tomography imaging algorithm.

Keywords: Rosetta, CONSERT, radar, tomography, FDTD, simulation

Investigation for the precise measurement method of lunar and planetary heat flow and development of heat flow probe

Yamato Horikawa^{1*}, Satoshi Tanaka², Naoya Sakatani³, Jun Takita¹, Kazunori Ogawa²

¹The University of Tokyo, ²Japan Aerospace Exploration Agency, ³The Graduate University for Advanced Studies

The precise measurement of lunar and planetary heat flow is an essential method for constraining their internal temperature distribution, thermal history, and material composition. Besides the Earth, the in-situ measurements were only conducted in the Apollo 15 and 17 missions on the Moon. About 20 years later from the Apollo missions, a high speed penetration probe (so-called penetrator), developed at Institute of Space and Astronautical Science in Japan, has an advantage that the heat flow measurements can be conducted at many sites at once mission. However, because the heat flow measurement devices on board a penetration probe including the probe of Apollo mission and penetrator are exposed on the regolith, they are easily influenced on the thermal distribution of the regolith varying from the heat conduction of the penetration probe. Therefore the heat flow measurement devices have the uncertainty for determining the planetary intrinsic heat flow value.

In this study, we investigate the thin heat flow probes which can be extended from surface of the penetration probe to a point indicating more intrinsic heat flow value of the planet (requirement of accuracy: better than 10%). On this presentation, we report the result of comparison investigation with the accuracy of heat flow from the measurement principle of thermal conductivity and thermal gradient and the numerical simulation based on the model of penetrator, and the accuracy of heat flow measured by the developed heat flow probe.

From the measurement principle and the numerical simulation, in case of the heat flow probe which has several sensor points, the two of their sensor points are tip of the probe which is the most accurate position of thermal gradient, and center of the probe which is the most accurate position of thermal conductivity. The accuracy of heat flow at these points is found to be 2.4% on the lunar regolith, and 1.9% on the martian regolith. In addition, we constrained the variety, length, and diameter of the probe material as considering the accuracy of heat flow and the strength of heat flow probe extending to regolith.

From restriction of development of heat flow probe, we made the heat flow probe of multiple sensor point, and conducted the experiment of heat flow measurement of glass beads at atmosphere pressure and vacuum. As a result, at atmosphere pressure, when the sensor point is from center to 3cm from center of the probe, we can accomplish the requirement accuracy of thermal conductivity (about 5%). When the sensor point is center of the probe, the best accuracy of thermal conductivity was determined to about 1.8%. On the other hand, at vacuum, comparing with the thermal conductivity by the heat flow probe and by line heat source method, the relative error of about 35-84% occurred when the sensor point is from 1cm to 3cm from center of the probe. Therefore the accuracy of thermal conductivity from the experiment of the heat flow probe was found not to be consisted with that from the measurement principle of thermal conductivity at vacuum.

To distinguish whether these error were caused by the glass beads or the heat flow probe, we measured rise profile in temperature of air which is more uniform distribution of thermal conductivity than that of glass beads. In the result, we found that the error at 1,2cm from center of the probe was caused by the probe, and the error at 3cm from center of the probe was caused by the glass beads. As future work, this error cause is required to discuss quantitatively to determine the measurement accuracy of heat flow probe at vacuum.

Keywords: heat flow, moon, planet, regolith

Effect of compressional stress on thermal conductivity of powdered materials under vacuum

Naoya Sakatani^{1*}, Kazunori Ogawa¹, Yu-ichi Iijima¹, Shoko Tsuda¹, Rie Honda², Satoshi Tanaka¹

¹Institute of Space and Astronautical Science, ²Kochi University

Lunar and asteroid surface is covered with powdered materials and planetesimals in the early solar system are considered to have consisted of powdered materials. Thermal conductivity of powdered materials is one of the essential parameters in order to examine thermal state or thermal evolution of these bodies. Especially under vacuum conditions, the thermal conductivity of powdered materials is known to be extremely low (order of 0.001 W/mK). Therefore, existence of such powders significantly affects the above problems. For example, to measure crustal heat flow on the moon, it is necessary to insert a heat flow probe. However, compaction of the regolith due to the inserting can change the thermal conductivity of the regolith from original one, which enlarges the error of the estimated heat flow (Grot et al., 2010). It is important to expect the degree of the compaction and correct the thermal conductivity values. In addition, Ogawa (2013) calculated thermal evolution of planetesimals composed of powdered materials. She showed that planetesimals as small as 10 km possibly experience melting or differentiation.

However, it is difficult to estimate the thermal conductivity value of the powder materials, because under vacuum it depends on various parameters such as particle size, density, and compressional stress. We have investigated the parameter dependence of the thermal conductivity of powder samples. In this presentation, we report the effect of compressional stress. It is one of the essential parameters in order to correct the heat flow values and to estimate the difference of the conductivity by planetesimals size (gravity) and the variation in the direction of the depth.

For the measurements of the stress dependence, we designed and fabricated a new experimental apparatus. The stress range we require is up to relatively low stress about a few tens kPa. To achieve this, we adopted a technique, in which six weights with known mass superimpose the powder sample by turns for controlling the compressional stress. Each weight suspended with strings at interval of 2 cm and they were moved up and down by an ultrasonic motor. Total mass of the weights was 7.5 kg, which corresponds to the maximum stress of about 18 kPa. Under such system, there was a sample container having two stress transducers with relatively low capacitance and a thermal conductivity measurement system by the line-heat source method. The sample was spherical glass beads of 0.1 mm diameter. Above apparatus was evacuated in the vacuum chamber and the thermal conductivity was measured without and with the weights.

As a result, the thermal conductivity was ranged from 0.003 to 0.008 W/mK and definitive trend that the conductivity increases with the compressional stress. This trend is considered to be due to increasing thermal conductance through elastically deformed and enlarged contact area between the particles.

The effective thermal conductivity under vacuum condition is defined as a sum of contributions of thermal conduction through the solid particles (so-called solid conductivity) and thermal radiation between particle surfaces (radiative conductivity). Because the observed trend is due to the variation of the solid conductivity, we subtracted the radiative conductivity for the same sample, which was determined by another experiment (Sakatani et al., 2013), from the measured conductivity and deduced the solid conductivity as a function of the stress. By fitting of these data by an appropriate function, we found that the solid conductivity depends on the stress with an exponent of 0.32 to 0.40. This value is compared with Hertzian theory that states the contact radius between spherical particles is proportional to the confined pressure with 1/3 exponent. This consistency strongly supports that the observed stress dependence is caused by the elastic deformation of the particles and that the solid conductivity is proportional to the contact radius.

Keywords: thermal conductivity, powdered materials, compressional stress, vacuum

Formation and thermal evolution of Ceres inferred from hydrothermal experiments and mineralogical analyses

Megumi MORI^{1*}, Yasuhito Sekine², KUWATANI, Tatsu², SHIBUYA, Takazo³, SIZUKI, Katsuhiko⁴, MASAKI, Yuka⁴

¹Dept. Earth & Planet. Sci., Univ. Tokyo, ²Dept. Complexity Sci. & Engr., Univ. Tokyo, ³Precambrian Ecosys. Lab., JAMSTEC, ⁴IFREE, JAMSTEC

The dwarf planet Ceres is the largest body in the asteroid belt and is frequently referred as one of the few protoplanets remaining in the inner solar system. Ceres' low density and spherical shape indicate that its interior is highly likely differentiated into a rocky core and water-rich ice mantle. Theoretical models of thermal evolution suggest that Ceres possibly underwent significant melting to explain the interior structure. These results further suggest that primitive minerals, such as olivine, would have been hydrothermally altered inside Ceres. The compositions of such secondary minerals may vary according to not only temperature but also the composition of aqueous solution, such as CO₂ abundances. Accordingly, the mineral assemblages on Ceres' surface would provide clues for understanding the timing of formation and chemical compositions of planetesimals that formed Ceres. Recent observations of Ceres suggested the possible presence of brucite, magnesium carbonates, Fe-rich serpentine, and magnetite on the surface. However, it remains unclear the temperature conditions and aqueous compositions that can account for the formation of these minerals.

In this study, we conduct hydrothermal experiments simulating chemical reactions that would have occurred in the interior of Ceres. In particular, we aim at investigating the effects of temperature and the amount of initial CO₂ on mineralogical and chemical compositions of secondary minerals formed from olivine. The experiments were conducted at temperatures of 200, 300, and 400°C and a pressure of 400 bar. We used powdered San Carlos olivine (Mg/(Mg/Fe)=0.9) as starting materials. Aqueous solution of 0.02% or 0.6% of NaHCO₃ (as a source of CO₂) and 1% of NH₃ was also used in the experiments. After the experiments, we collected rock residues and analyzed their mineralogical and chemical compositions using a XRD and SEM-EPMA, respectively.

Our experimental results suggest that temperature dependency of oxidation of Fe(II) to magnetite strongly affects the mineralogical and chemical compositions of secondary minerals. Magnetite formation proceeds efficiently at 300°C, which diminishes partitioning of Fe(II) into secondary minerals resulting in low Fe/Mg ratios in serpentine. At 200°C, serpentines with relatively high Fe/Mg ratios and a very small number of magnetite were found in rock residues. These results suggest that oxidation of Fe does not proceed efficiently at 200°C, leading to partitioning of Fe(II) into secondary minerals during serpentinization. Brucite was found in rock residues formed only at 300°C. There are few brucite in rock residues formed at 200°C. Because olivine is thermodynamically stable, any alteration minerals were not formed at 400°C.

Initial amount of CO₂ also affects the compositions of secondary minerals via carbonate formation. Brucite tends to be abundant under a low CO₂ condition in rock residues, whereas few brucite are formed under a high CO₂ condition. Serpentines with relatively high Fe/Mg ratios were produced under a high CO₂ condition. These results suggest that efficient carbonate formation under a high CO₂ condition prevents from formation of brucite and results in formation of serpentines with relatively high Fe/Mg ratios.

In our experiments, we cannot find a single condition, under which the secondary mineral assemblages found on Ceres' surface are reproduced. Especially, we found that brucite tends to be formed more efficiently under lower CO₂ conditions. In contrast, formation of Fe-rich serpentine prefers lower temperature (~200°C) and higher CO₂ conditions. These results suggest that Ceres' surface would be compositionally heterogeneous owing to geological activities, such as impact cratering. Our experimental results suggest that formation of brucite requires moderate temperatures, such as 300°C. To achieve such temperatures, Ceres is required to have been formed at ~200-300 My after the formation of CAIs.

Keywords: hydrothermal reactions, Ceres, early solar system, mineralogical analysis

Experimental study of ice lens formation and application for planetary surface environment

Tomotaka Saruya^{1*}, REMPEL, Alan W.², Kei Kurita¹

¹Earthquake Research Institute, University of Tokyo, ²University of Oregon

Ice lenses are formed by the migration and freezing of water in partially frozen state during soil freezing. Nucleation and growth of ice lenses cause the upwards displacement of ground surface and formation of periglacial landforms. Beyond the terrestrial environment, similar processes are believed to occur in planetary environment. For example, periglacial landforms or high-purity ice are observed at the Phoenix landing site on Mars. Formation of ice lenses is complicated phenomena including heat and mass transport. Several theoretical models address its physical processes in terrestrial environment, however, many questions still remain for the formation of ice lenses. Especially, experimental constraints are not enough. We performed systematic cooling experiment using granular materials to observe the behavior of ice lenses. Our experimental results demonstrate the relationships between the behavior of ice lenses and particle size, temperature conditions and force balance. We also compared our experimental results to numerical model of ice lens formation that focuses on the force balance of thermomolecular force and hydrodynamic force. As a results of comparison, qualitative consistency is obtained, however, important quantitative differences existed. We developed initial numerical model using kinetic effect around particle surface and obtained good agreement.

Application experiments that simulate planetary surface environments are also performed (e.g., low pressure environment, carbonated water etc.) and we observed different behaviors as compared with basic experiments.

In this presentation, we report the comparison between the experimental results and theoretical model and application experiment under simulated planetary environment.

Keywords: ice lens

Large scale transportation of materials and chemical evolution in protoplanetary disc

Hiroko Nagahara^{1*}

¹Hiroko Nagahara

Introduction: Large scale material transport in protoplanetary disks has been proved by finding of the high temperature components in comet Wild 2, and it has been supported by physical consideration (e.g., Ciesla, 2009). Meteorites show a wide range of variation of oxygen isotopic compositions, which have been thought to be inherited from the precursor molecular cloud. However, recent high precision by ion microprobes has revealed that the variations are a mixture of isotopic mixing and mass-dependent isotopic fractionation [e.g., Tenner et al., 2012].

Model: In order to understand material transport and oxygen isotopic characteristics recorded in meteorites in a protoplanetary disk, we have developed a model that describes mixing of two components, one transporting outward from the inner edge and one transporting inward by accretion of a protoplanetary disk with different oxygen isotopic compositions. We assume that the proto-sun had ¹⁶O-rich composition as suggested by the solar wind component captured by the Genesis mission, which is represented by refractory inclusions and forsterite grains in primitive chondrites. The planetary composition is represented by the Earth with slight deviation as Mars and asteroids. The materials from outer region were assumed to have oxygen isotopically heavy composition, which we tentatively assume to be that observed in magnetite in a unique carbonaceous chondrite.

The model investigates isotopic trajectory of solid materials condensed at high temperature region with proto-Sun composition, which changed the composition by isotopic exchange in gas with heavy oxygen isotope composition. The solid materials cool exponentially with time. The system has the composition of the solar abundance elemental ratios except for H₂O as a source of heavy oxygen isotope in gas; isotopic exchange is temperature dependent; material transport flux is a steady state. The model contains two free parameters; one is cooling rate and the other is isotopic mixing rate.

Results and Discussions: The solids become isotopically heavier with time due to isotopic exchange, and the time of the increase is shorter and the final composition becomes heavier when the mixing rate is large. The time of the increase of the heavy isotope becomes later and the final composition becomes isotopically lighter with decreasing mixing rate. Considering that the planetary composition of oxygen isotopes is $\delta^{18}\text{O} = \text{zero}$ by definition, the most plausible mixing rate is obtained. We have confirmed that the mixing lines on the three oxygen isotopic plot are straight for both solids and gas, which means that the solid changed its composition from -50 to 0 permil and that the gas from +200 to 0 permil.

A plausible range of the mixing rate was obtained for a range of cooling rates. The mixing ratio of solids with light oxygen and gas with heavy oxygen and cooling rate are linearly related in logarithmic plots. In other words, more abundant low temperature component with heavy oxygen is required if the solid materials cool rapidly. The model results are converted to the real scale for forsterite grains condensing in light oxygen gas, which moves outward, cools, and exchanges oxygen isotopes with ambient gas with heavy composition. Cooling rate of the model corresponds to advection or diffusion rate at the midplane and the mixing rate corresponds to the ratio of inward flux of isotopically heavy water ice to outward flux of high temperature condensates with light oxygen isotopes. Larger values of cooling rate and mixing rate may be realized at the early stage of disk evolution.

In summary, planetary oxygen isotopes were achieved through the evolution of the disk due to larger inward and outward transportation of materials and ice at the early stage and smaller transportation at the later stage.

Keywords: protoplanetary disc, solid materials, transportation, oxygen isotope

Disk lifetime of protoplanetary disks surrounding intermediate-mass stars in the inner Galaxy

Chikako Yasui^{1*}, Naoto Kobayashi¹, Masao Saito², Alan T. Tokunaga³

¹University of Tokyo, ²National Observatory of Japan, ³University of Hawaii

Disk lifetime is one of the most important parameters which can control planet formation. The disk lifetime has been estimated by various studies to be $\sim 5\text{--}10\text{Myr}$. However, this value is applicable only to studies for the solar metallicity. For a thorough understanding of planet formation, the disk lifetime should be determined in other (metallicity) environments. This may impose a strong constraint on the disk evolution mechanisms and the planet formation processes.

We previously derived disk fraction in the outer Galaxy (~ 15 kpc from the center of the Galaxy), which is known to be the low-metallicity environments ($\sim 1/10$ solar metallicity), and found that disk lifetime is much shorter ($\sim 1\text{Myr}$) than that of the solar metallicity. For the next step, we derived the disk fraction of intermediate-mass stars in the inner Galaxy ($\sim 4\text{kpc}$ from the center of the Galaxy), which is a high-metallicity environment ($\sim 3\text{x}$ solar metallicity), and found a relatively high disk fraction for a cluster with the age of $\sim 20\text{Myr}$. This cluster is older than the disk lifetime in solar metallicity clusters, and this suggests that the disk lifetime is much longer in higher metallicity environments. In this talk, I am going to discuss metallicity dependence of disk lifetime in a wide metallicity range from 0.1 to 3 times solar metallicity

Keywords: protoplanetary disk, metallicity, planet formation

Concentration of dust aggregates at the snow line

Sin-iti Sirono^{1*}

¹Nagoya University

Planetesimal formation process is still an important, unresolved problem in planetary formation. There are two major problem in the planetesimal formation. One is the large impact velocity induced by radial drift of dust aggregate. This might lead to fragmentation of aggregates. The other is decrease of solid mass due to the radial drift. Here I propose a new scenario of planetesimal formation, focusing the sublimation of H₂O ice from infalling dust aggregates.

The temperature of a dust aggregate increases as it infalls. The temperature increase causes the sublimation of H₂O ice from an icy dust aggregate. The sublimation of the H₂O ice produces a bump of gas pressure distribution. Around the bump, the pressure gradient changes its sign, and the infalling of a dust aggregate stops. Then the number density of the aggregates increases, and relative impact velocity between aggregates decreases. I show that planetesimals are formed quite quickly due to the concentration of the dust aggregates.

Keywords: grain aggregate, planetesimal, sublimation

Three dimensional shapes and internal structure of chondrules from Allende CV3 chondrite

Ayaka Tsuda¹, Keisuke Nishida^{1*}, Eiichi Takahashi¹, Taishi Nakamoto¹, Tetsuya Yokoyama¹, Osamu Sasaki², Kanou Harumasa², Yasuhiro YANAGIDA³, Satoshi Okumura³, Michihiko Nakamura³

¹Earth and Planetary Sciences, Graduate School of Science and Technology, Tokyo Institute of Technology, ²The Tohoku University Museum, ³Department of Earth Science, Graduate School of S

Origin of chondrules in meteorite is still controversial issue. Miura and Nakamoto have developed a shock-wave heating model for chondrule formation in a series of papers (Miura et al., 2002, 2005, 2008). According to the model, systematic relation would be expected between 3D shapes and internal structure of chondrules. Using X-ray CT at SPring-8 synchrotron, Tsuchiyama et al. (2003) measured 3D shapes and internal structure of 47 chondrules separated from Allende CV3 meteorite. They found that 4 out of 20 chondrules show prolate-shape (like a rugby-ball) and others show near spherical shapes. The prolate-shape could be explained by high-rotation during the shock wave heating episode, while the shock wave heating model predicts oblate-shape (like a pancake) chondrules without rotation. However, oblate-shaped chondrules were not observed in Tsuchiyama et al's study, most probably due to small number of samples analyzed.

In order to clarify 3D shapes and internal structure of chondrules, we have separated 180 chondrule grains from the Allende meteorite by a freeze-thaw method and hand picking. The internal structure of chondrules was investigated using the X-ray CT apparatus (Scan Xmate-D180RSS270) recently installed at the Museum of Natural History, Tohoku University. The 3D shape of chondrules was examined by an optical device newly developed (Nishida et al. JPGU 2013).

As presented in Fig. 1, the 3D shapes of chondrules show wide distribution consisting of true spheres, prolate-spheres and oblate-spheres. Note that 25 chondrules with nearly spherical shapes were not examined for X-ray CT to save time. About 60% of the measured chondrule grains were omitted in Fig. 1 because of imperfect shapes due to destruction or presence of matrix. Chondrules with porphyritic texture distribute in all shape categories. Chondrules with granular texture (lower melting degree than porphyritic) also show nearly homogeneous distribution. Chondrules with barred olivine texture (quenched from superheated melt) show a distribution between true sphere and oblate-shape. Implication of the 3D shapes and internal texture of chondrules will be discussed from the shock-wave heating model.

Keywords: Allende, Chondrule, X-ray CT, Three-dimensional shape, Shock-wave heating model

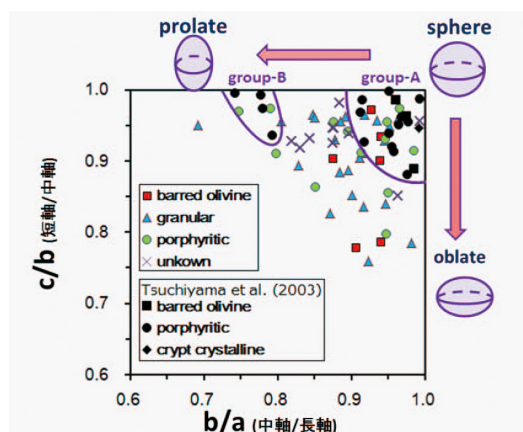


Fig.1 3D shape and internal texture of chondrules in Allende CV3 chondrite

Planetary Migration in Dust-Rich Disks

Kou Yamada^{1*}, Satoshi Inaba²

¹Graduate School of Political Science, Waseda University, ²School of International Liberal Studies, Waseda University

There are still serious problems in the theory of planet formation. One of the problems is how to keep protoplanets with Earth-masses in a disk for a sufficiently long time until the disk gas is dispersed. A protoplanet growing in a disk interacts with a gas disk gravitationally and, as a result, changes the radial distance from the central star. This process is called the type I migration of a protoplanet. A variety of structures of extrasolar planetary systems might be a natural outcome resulted from the type I migration. The corotation torque and the Lindblad torque act on a protoplanet, leading to the type I migration of the protoplanet. The migration velocity of the protoplanet is determined by the sum of the torques. Recently, Yamada & Inaba (2012) showed that the magnitude of the torques depends on a thermal structure of a disk. The positive corotation torque acting on a protoplanet in a disk inside of the ice line becomes large enough to cancel the negative Lindblad torque. Protoplanets might accumulate at the location of the ice line of a disk with small viscosity.

Once dust particles grow, they move in a disk interacting with gas. Particles lose angular momentum and migrate inward toward the inner region of a disk. The particle density in the inner region of a disk is increased with time. Birnstiel et al. (2012) studied the evolution of the particle surface density considering the growth and fragmentation of particles and the radial motion of the particles as well. They showed the greatly increased particle-to-gas ratio in an inner region of a disk with small viscosity in 1Myr. We study the effect of particles on the type I migration of a protoplanet. We compare the torques acting on a protoplanet by disks with and without dust particles. Parameters in this model are particle radius (0.1mm to 1cm) and particle-to-gas mass ratio (0.01 to 0.1). We find that the magnitude of the positive corotation torque acting on a protoplanet is dependent on the particle size and increases with an increase in the particle-to-gas mass ratio. A protoplanet may be prone to migrate outward in dust-rich disks.

Keywords: type I migration, density wave, dust, planetary system, corotation torque, gravitational interaction

Detection of magnetic anisotropy of a single grain crystal orientated to investigate the origin of dust alignment.

Chiaki Uyeda^{1*}

¹Graduate School of Science, Osaka University

Distribution of magnetic fields in inter- and circum-stellar regions is commonly estimated from the observation of visible and infrared polarization, which is caused by the magnetic alignment of the dust particles. The origin of alignment in the diffuse interstellar region is explained by a paramagnetic relaxation model assumed for the grains. However in the high-density regions, efficiency of the above mechanism is still unclear since the dust is in thermal equilibrium with the gas molecules. An alternative possibility was proposed on the mechanism, which was based on the balance between the rotational Brownian energy and the magnetic anisotropy energy induced in the dust. Here the magnetic anisotropy are caused by paramagnetic anisotropy and/or by diamagnetic anisotropy.

A new principle to detect magnetic anisotropy of a small crystal is experimentally examined by measuring the anisotropy of paramagnetic apatite crystals having sub-millimeter sizes. The new method is based on a rotational oscillation of magnetically stable axis with respect to field direction. Here the crystal is released in a diffused area using a short microgravity condition. The method is hence free of mass measurement; anisotropy can be measured for a limitlessly small crystal grain, in condition that the oscillation is observable. In a conventional method to detect anisotropy, existence of a sample holder and difficulty of mass measurement had prevented the detection of small samples. A chamber-type drop shaft was newly developed to observe the field-induced oscillation; duration of microgravity was below 0.6s. Volume of drop box was as small as 100 cm^3 , weight was below 1kg. The compact size of apparatus was realized by introducing a small NdFeB magnetic circuit with dimensions of 2.5 cm x 2.0 cm x 0.6 cm ($B < 0.6 \text{ T}$).

Rotational oscillation was observed for 4 apatite crystals with different sizes, and the anisotropy value was determined in terms of a formula established for the period of harmonic oscillation. The obtained values of anisotropy both agreed fairly well with the published values. It was confirmed from the experiment that the position of the sample stage, located at the center of N and S pole, was effective to spontaneously release the sample by an attractive field gradient force. In previous micro-g experiments, release of sample was often prevented by a Coulomb attractive force between sample and holder deriving from the electric charges. The above-mentioned field-gradient force is effective to reduce the interference of the attractive force.

The mass independent property of the above oscillation was examined in wide range of sample size; namely between 1.0 and 0.1mm in diameter. The present technique of observing anisotropy of a sub-millimeter-sized crystal is a step toward realizing anisotropy measurements of micron-sized grains. Precise anisotropy values of single micron-sized grains can be used to examine the validity of a dust alignment model based on magnetic anisotropy energy induced in the dust particles.

[1] C.Uyeda et al: Jpn. Phys. Soc. Jpn. 79, 064709 (2010).

Keywords: magnetic alignment, rotational oscillation, dust alignment, apatite, diamagnetic anisotropy, micro-gravity

Orbital evolution of eccentric, gas-accreting protoplanets

Akihiro Kikuchi^{1*}, Arika Higuchi¹, Shigeru Ida¹

¹Department of Earth and Planetary Science, Graduate School of Science and Technology, Tokyo Institut

Distant giant exoplanets with nearly circular orbits have recently been detected by direct imaging observations. The formation of these planets is not accounted for by the standard scenario of planet formation. According to this scenario, a protoplanet is first formed by the accretion of planetesimals. Once its mass exceeds a critical mass, runaway accretion of gas starts and it becomes a giant planet. However, at large distances from the central star, the long timescale for the accretion of planetesimals prevents any protoplanet from reaching this stage before the gas in the disk has disappeared. Another scenario has thus been proposed by Nagasawa (2008): it involves a formation of a giant planet close to the star followed by scattering by another giant planet. The planet that has been scattered outward can thus reach large distances, but not on a circular orbit.

We propose a new scenario for the formation of distant and circular giant planets: We first assume that while still in the gas disk phase, a protoplanet is scattered outward by an inner giant planet. We then show that the orbit of the protoplanet can become circular because of a damping of the eccentricity due to its accretion of gas. Since the sum of orbital and collisional energy is conserved, the semimajor axis must decrease while the planet accretes mass.

We provide an analytical solution to the orbital evolution assuming that the gas accretion rate remains constant along the planet's orbit, but can evolve slowly as a function of the planetary mass. We average the energy and angular momentum provided to the planet by gas accretion over each orbit to obtain differential equations for the orbital elements. The time-evolution of the semimajor axis and eccentricity are obtained by integrating of these equations.

We find that even highly eccentric protoplanets ($e=0.99$) can evolve into nearly circular orbits by gas accretion. When evolving from a protoplanetary mass of 10 Earth masses to a mass of Jupiter, we find that the final eccentricity is always less than 0.05. The inward migration of the protoplanet directly depends on the eccentricity, and it limited to a semi-major axis of about half its initial value. This scenario therefore can explain the orbits and masses of the giant exoplanets discovered by imaging techniques.

Finally, we examine the orbital evolution of a giant planet in a truncated gas disk. We derive a relation between the disk radius and the final semimajor axis of the giant planet. We will discuss the relation in detail and apply it to various disk model.

Keywords: exoplanet, distant jupiters in circular orbits, planetary formation, gas accretion, orbital evolution

Gap formation by a planet in a protoplanetary disk considering the change of disk rotation law

Kazuhiro Kanagawa^{1*}, Hidekazu Tanaka², Takayuki Muto³, Takayuki Tanigawa², Taku Takeuchi⁴

¹Department of cosmosciences, Gradient School of science, Hokkaido University, ²Institute of Low Temperature Science, Hokkaido University, ³Division of Liberal Arts, Kogakuin University, ⁴Department of Earth and Planetary Sciences, Tokyo Institute of Technology

In a protoplanetary disk, earth-sized or larger planets interact gravitationally with the disk and, by this interaction, they can reduce the disk surface density around their orbit. This makes gaps in the gaseous disk. For larger planets, their gaps terminate the disk gas flow across orbits of the planets, which is thought to explain the formation of the transition disks with the inner hole. Many transition disks with inner holes or gap structures have been observed.

In the near future, more detail structures of transition disks will be revealed by the direct imaging by the Atacama Large Millimeter/submillimeter Array (ALMA).

However, the formation of gaps and inner hole by planets is still theoretically uncertain process, and there is no quantitative model to explain the relation between the planet mass and the shape and depth of gaps. The goal of our study is the construction of a formation model for the inner hole and gap around a planet, by using one-dimensional viscous accretion disk model with the disk-planet interaction. In previous studies on the gap formation, the change in the disk rotation law due to the gaseous pressure gradient has been neglected. However, owing to a steep surface density gradient in the gap, the deviation from the Keplerian rotation law can be remarkably large. Moreover, the surface density profile in the gap is strongly influenced by the deviation of the disk rotation law.

In this study, we examine the surface density profile of the gap in a self-consistent way, by taking into account the deviation of the disk rotation law due to the steep surface density gradient. Our results are as follows;

(1). The change of rotation law promotes the viscous angular momentum transfer in the gap, and, as a result, the gap becomes shallower than the evaluation by previous studies. This effect is stronger for a deeper gap, and the depth of the gap is significantly reduced.

(2). Owing to the significant change of rotation law for a deep gap, the Rayleigh criterion that is stable condition for the rotation disk can be broken. In this case, the structure would be shift to the marginally stable state for the Rayleigh criterion (Tanigawa & Ikoma 2007). Solving the gap structure including the breaking the Rayleigh criterion, we find that the viscous angular momentum transfer is promoted by the breaking of the Rayleigh criterion, and then, the depth of the gap is further reduced.

In addition to above results, I want to talk about the comparison between the result of numerical fluid simulation and the results of our model.

Keywords: protoplanetary disk, disk-planet interaction, disk evolution, gap formation

Numerical simulations and analytical evaluations of type I migration in disks heated by the stellar irradiation

Naohiko Maeshima^{1*}, Sei-ichiro WATANABE¹

¹Division of Earth and Planetary Sciences, Graduate School of Science, Nagoya University

Planets are formed in protoplanetary disks and migrate radially by gravitational interaction with the disk gas. The type I migration was problematic because planets rapidly fall into the central stars in the isothermal disks. However, recent studies revealed that in the adiabatic disks planets can migrate outward in the region where the entropy gradient is negative (Paardekooper & Mellema 2006; Baruteau & Masset 2008; Paardekooper & Papaloizou 2008). There is a study calculating type I migration in the non-isothermal disks (Lyra et al. 2010), but they does not considered the stellar irradiation as the mechanism of the disk heating.

We studied the type I migration in the non-isothermal accretion disks heated by the central star using numerical calculation. As mechanisms of the disk heating, we considered both the viscous heating and the stellar irradiation. We find that 'equilibrium radii', where the torque exerting on a planet becomes zero, moves inward in the disk with the timescale of disk evolution, and planets move with the equilibrium radii until gas densities decrease so low that the planets stop migration. One of the equilibrium radii exists on the region where main heating mechanism changes from viscous heating to stellar irradiation and that the terminal position of a comoving planet with mass of $10 M_E$ is about 1AU. The terminal position is less sensitive to parameters such as turbulent viscosity, mass flux of photoevaporation, and mass of the central star. On the other hand, the planets migrating from the relatively inner disk arrive at the vicinity of the central star (disk inner edge). If core instabilities occur on the planets, hot Jupiters are formed. We also obtain analytical expression of equilibrium radii and terminal positions of migrating planets, which coincides well with the results of our numerical simulations.

We compare our results with the distribution of the semimajor axes of observed exoplanets. Especially many giant planets ($>100M_E$) have been observed in the regions inside 0.1AU and outside 1AU, and the number ratio of planets is about 3:5. A relatively small number of exoplanets are observed between the two regions. Such a bimodal distribution of semimajor axes of exoplanets can be explained by the results of our simulation. We will discuss the ratio of the number of planets in the two regions quantitatively.

References

- Baruteau, C., & Masset, F. 2008, *ApJ*, 672, 1054.
- Lyra, W., Paardekooper, S.-J., & Mac Low, M.-M. 2010, *ApJ*, 715, L68.
- Paardekooper, S.-J., & Mellema, G. 2006, *A&A*, 459, L17.
- Paardekooper, S.-J., & Papaloizou, J. C. B. 2008, *A&A*, 485, 877.

Keywords: type I migration, protoplanetary disk, exoplanet

Effects of Evaporation of Hot-Jupiters on Exoplanets Population

Hiroyuki Kurokawa^{1*}, Taishi Nakamoto¹

¹Tokyo Institute of Technology

As the number of observed exoplanets increases, statistical discussions have been possible. It has been pointed out that there are correlations between semi-major axes (or orbital periods) of planets and planetary masses, surface gravities, or densities (Mazeh et al., 2005; Southworth et al., 2007; Jackson et al., 2012). One possible mechanism to account for the correlations is XUV-driven atmospheric escape due to the heating of upper atmosphere by stellar XUV (e. g., Lammer et al., 2003; Jackson et al., 2012).

Previous works which test the hypothesis neglected thermal cooling and evolutions of planetary radii or densities due to mass-loss. Also, the energy-limited escape was simply assumed. However, the changes of planetary radii and densities can result in a runaway mass-loss (Brafte et al., 2004). The Roche-lobe overflow might contribute to mass-loss in such a runaway regime. In addition, under an intense XUV environment which is possible in earlier stages of a host star, the thermal escape is in the recombination-limited regime (Murray-Clay et al., 2009; Owen and Jackson et al., 2012), not in the energy-limited regime as assumed in previous works on mass-loss evolutions. In this study, we develop a model to calculate the thermal evolution and the mass-loss evolution simultaneously taking the Roche-lobe overflow and the recombination-limited escape into account.

As a result, we show that a total evaporation of an envelope occurs for planets orbiting close to the host star (~ 0.015 AU for a Jupiter-mass planet) and the evaporation is in the recombination-limited regime, not in the energy-limited regime. The mass-loss results in an expanding of the planetary radius and it is followed by the runaway mass-loss. The mass-loss evolution finally causes the Roche-lobe overflow. Because it strongly depends on the initial mass of the planet whether the planet experiences the runaway mass-loss or not, we can define a critical mass for a planet to lose whole envelope as a function of the semi-major axis. We show a comparison of the semi-major axis - critical mass relation obtained by our calculation and the observed population of exoplanets. Our results for Hot-Jupiters which have a small core of ~ 10 Earth mass are consistent with the observation.

Keywords: exoplanet, atmospheric escape, gas planet, Hot-Jupiter, stellar XUV

Theoretical threshold mass and radius for close-in low-mass water-rich super-Earths: Implications for the main composition

Kenji Kurosaki^{1*}, Masahiro Ikoma², Yasunori Hori³

¹Tokyo Institute of Technology, ²Tokyo University, ³National Astronomical Observatory of Japan

Recent progress in observational technique has enabled us to find many exoplanets that have as small as several to several ten Earth masses and/or Earth radii (hereafter super-Earths). We can obtain the planetary mean densities from measured planetary masses and radii and thereby infer planetary compositions. It has been revealed that low-mass planets with short orbital periods (close-in planets) are diverse in composition. Despite of closeness, there are a significant number of close-in planets that have the potential to be mainly composed of water components (e.g., GJ1214b). Planetary composition is important to understand the planet's evolution and origin. I investigate mass-radius relationships for water-rich close-in planets, including the effects of thermal evolution and mass loss. Since close-in planets are strongly irradiated, they are rather hot and also experience mass loss. Nevertheless, impacts of those effects on the mass-radius relationships for water-rich planets have not been investigated previously. Through the investigation, I intend to derive threshold values for planetary mass and radius and constrain observations that can possess water components. I have calculated the interior structure and evolution of close-in water-rich planets, including the XUV-driven energy-limited hydrodynamic escape. I assume that the planet, orbiting a solar-type star, has three-layer structure: a water-vapor atmosphere, a water mantle and a rocky core from top to bottom. I have realized that the mass loss due to the intense stellar-XUV irradiation has a significant impact on evolution of close-in planets. In particular, water envelopes of the planets with mass of less than a few Earth masses, depending on distance from their host stars, are completely stripped off. I have derived a threshold value of the planet's initial mass below which the planet loses its water mantle completely. This threshold has been obtained as a function of the semi-major axis and other input parameters. The theoretical model of the structure and evolution of close-in water-rich planets in this dissertation predicts the domains in mass-period and radius-period distributions where naked rocky planets or water-rich planets are likely to be detected. This provides an essential piece of information for understanding the origin of close-in low-mass planets.

Keywords: Super-Earth, Mass loss, Interior structure

Formation and stability of habitable moons around extrasolar giant planets

Takao Sato^{1*}, Takanori Sasaki¹

¹Department of Earth and Planetary Science, Graduate School of Science and Technology, Tokyo Institut

Since the discovery of planets in other systems, the question of whether these extrasolar planets are habitable has become relevant and addressable. However, it has been observationally difficult to catch an Earth-sized planet in the habitable zone. On the other hand, RV observations have shown large amount of giant planets exist in the habitable zone. In this paper, we focus on the exomoons around these extrasolar gas giants.

Williams et al. (1997) estimated the lower limit of satellite's mass to be habitable as 0.1-0.2 Earth masses. We examine the formation and orbital stability of satellites that has these masses around gas giants in the habitable zone. We showed the satellites tend to be rocky ones because of the high temperature profile of circum-planetary disks for massive gas giants. We also showed the orbits of these satellites are stable against type II migration of central planets and long-term tidal effect from the planets. Therefore, extrasolar giant planets in the habitable zone have a high probability of bringing "habitable moon" with.

Keywords: habitable moon, exoplanet, exomoon, satellite formation, orbital stability

Geological study on the formations of grooves on Phobos: Results of image analysis

Hiroshi Kikuchi^{1*}, Hideaki Miyamoto¹

¹The University Museum, The University of Tokyo

Phobos and Deimos have been imaged by Viking orbiter, HRSC onboard Mars Express, and HiRISE onboard Mars Reconnaissance orbiter. About 3000 high-resolution images of Phobos have been acquired, which indicates that Phobos becomes one of the most densely-imaged small solar system bodies. The purpose of our study is to understand formational and evolutionary processes of small bodies through image analysis.

One of the most distinguished features on the surface of Phobos is the lineally surface structure, which is most commonly called as a groove. Grooves are found on many small solar system bodies, however, their formational processes has not been explained.

Some formational processes of grooves on Phobos have been proposed, such as (1) the faults vents caused by tectonic forces [1] and (2) the secondary craters due to a large impact on either Phobos or Mars [2]. However, neither hypothesis satisfies findings from all of the observational or theoretical studies.

In this study, we carefully analyze high-resolution images of Phobos and identified 515 grooves, whose locations are carefully mapped out on the numerical shape-model of Phobos. At a result, we find that many grooves have rims, which support the view that the grooves on Phobos are related to impact events. We also make a histogram of the lengths of the grooves, where those more than 5km can produce reliable information.

We also map the locations of craters more than 20km in diameter on three regions to determine the crater densities, which are below geometric saturation at any regions. In particular the high-latitude region has a low crater density. We find that the crater size frequency on sub-Mars is similar to that on Anti-Mars. We also map the distributions and the size of boulders on the surface. As a result, the size of many boulders is about 20m diameter, and many boulders can be identified on the equatorial region. Additionally we discover ridges whose formative factor cannot be explained. These analysis results deny existing hypotheses. In this presentation, we will show our new hypothesis that the origin of grooves is the impact from asteroids can explain these analysis results coherently.

Reference

- [1] Soter, S. and Harris, A., 1978. *Nature* 268, 421-422
- [2] Murray, J.B., Iliffe, J.C., 2011. *Geomorphology. Geol. Soc. Spec. Publ.*, London, pp.21-41
- [3] Kenneth, R.R., James, W. H., 2013. *Planetary and Space Science*, 69-95

Numerical models of thermal convection in the mantle of super-Earths

Chihiro Tachinami¹, Masaki Ogawa^{2*}, Masanori Kameyama³

¹Department of Earth Planetary Sciences, Tokyo Institute of Technology, ²Department of Earth Science and Astronomy, University of Tokyo at Komaba, ³Geodynamic Research Center, Ehime University

Numerical models are developed for thermal convection of compressible fluid in a deep mantle with the ratio of its depth to the thermal scale height D much larger than 1 to understand the nature of mantle convection in super-Earths. The viscosity is constant and the Prandtl number is infinite. A linear stability analysis shows that thermal convection is possible in super-Earths only when the thermal expansivity significantly decreases with increasing pressure, as is the case for the real mantle materials; thermal convection is totally inhibited when the thermal expansivity is constant. A systematic numerical simulation carried out to clarify the Nusselt number-Rayleigh number relationship shows that the efficiency of convective heat transport decreases by a factor of up to 2 as D increases. The Nusselt number may not be high enough to extract all the heat generated in the mantle by heat producing elements, and it may be difficult to sustain core-dynamo in super-Earths. Our numerical experiments also show that the Nusselt number significantly depends on the surface temperature. The mantle evolution may depend more strongly on the surface environment in super-Earths than it does in the terrestrial planets of our solar system.

Keywords: super-Earth, mantle convection, adiabatic compression, numerical simulation

Rheological structure in Venus and implication to its surface tectonics

Shintaro Azuma^{1*}, Ikuo Katayama¹, Tomoeki Nakakuki¹

¹Hiroshima University, Department of Earth and Planetary Systems Science

Venus has been regarded as a twin planet to the Earth, because of density, mass, size and distance from the Sun. However, the Magellan mission revealed that plate tectonics is unlikely to work on the Venus [1][2]. The plate tectonics is one of the most important mechanism of heat transport and material circulation of the Earth, consequently, its absence might cause the different tectonic evolution between Earth and Venus. Rheological structure is a key to inferring mantle structure and convection style of planet interiors because the rock rheology controls strength and deformation mechanism. In previous study, the behavior of Venusian lithosphere has been inferred from the power-law type flow law of dry diabase [3]. They indicated that lower crust can be weaker than upper mantle, which might result decoupling at the crust-mantle boundary (Moho depth) and mantle convection without crustal entrainment. However, the power-law creep cannot be applicable to infer the rheological structure at Moho depths, because the dislocation-glide control creep (Peierls mechanism) is known to become dominant at relatively low temperatures in materials with a relatively strong chemical bonding such as silicates [4]. In this study, we conduct two-phase deformation experiments to directly investigate rheological contrast between plagioclase (crust) and olivine (mantle) and discuss the difference between these planets in terms of rheological behaviors. Moreover, one-dimensional numerical calculation is performed to evaluate the influence of strength contrast to the decoupling of deformation rate at the Moho. Our experiments using solid-medium deformation apparatus directly determine the relative strength between plagioclase (crust) and olivine (mantle) without any extrapolating of flow law. The experimental conditions were ranging 2GPa and 600-1000 degrees under dry conditions. In one-dimensional numerical calculation, three models were prepared; each model is distinguished in rheological structure. First model has no strength contrast at Moho, second and third models have double-digit difference and four-digit difference in viscosity each at Moho. And we observed difference of the surface velocity at each model when it is assumed that the velocity at the bottom (100km depth) is 20 cm/year and stress value is constant (=100MPa) at each depth in calculations.

The experimental results show that olivine is expected to always be stronger than plagioclase. This result contradicts to that inferred from power-law creep of olivine and plagioclase, suggesting that Peierls mechanism could be dominant deformation mechanism in both olivine and plagioclase at relatively low temperatures. In the case of the Earth, rheological structure of oceanic lithosphere is constrained well by Byerlee's law and power-law type flow law [5]. The oceanic crust and mantle lithosphere are strongly coupled mechanically because the Moho has no strength contrast, so that they could move and subduct together into the deep. In contrast, our experimental results imply that large strength contrast exists at Moho in Venus, resulting decouple of the motion between the crust and mantle lithospheres because the weak lower crust acts as a lubricant. Also one-dimensional numerical calculations show us that the surface velocity becomes more sluggish in the model which has larger strength contrast (from two-digit to four-digit difference in viscosity) at Moho. Therefore the crustal part is less likely to be involved to mantle convection when strength contrast gets larger and larger. [1] Kaula, W. M. & Phillips, R. J., *Geophys. Res. Lett.* 8, 1187 (1981). [2] Turcotte D. L., Morein G., Roberts D., & Malamud B. D., *Icarus* 139, 49-54 (1999). [3] Mackwell, S. J., Zimmerman, M.E. & Kohlstedt, D.L., *J. Geophys. Res.* 103, 975-984 (1998). [4] Tsenn, M. C. & Carter, N. L., *Tectonophys.* 136, 1-26 (1987). [5] Kohlstedt, D. L., Evans, B. & Mackwell, S. J., *J. Geophys. Res.* 100, 17,587-17,602 (1995).

Keywords: plagioclase, olivine, venus, relative strength, deformation experiment, tectonics

Laser shock compression experiments for precompressed Methane in Mbar regime

Tsuyoshi Ogawa^{1*}, Norimasa Ozaki¹, Marius Millot³, Takayoshi Sano², Yuto Asami¹, Syotaro Iketani¹, Hiroyuki Uranishi¹, Mika Kita¹, Yoshihiko Kondo¹, Yuya Sato¹, Kazuki Nakatsuka¹, Kohei Miyanishi¹, Yang Tsung-Han¹, Raymond Jeanloz³, Burkhard Militzer³, Gilbert W. Collins⁴, J. Ryan Rygg⁴, Jon H. Eggert⁴, Philip Sterne⁴, Youichi Sakawa², Ryosuke Kodama¹

¹Graduate School of Engineering, Osaka University, ²Institute of Laser Engineering, Osaka University, ³University of California Berkeley, ⁴Lawrence Livermore National Laboratory

The properties of methane at high density and temperature are of crucial interest for understanding the interiors of many giant planets, and the origin of their strong magnetic fields, as CH₄ is typically considered to represent 25 % of the planet's icy layer. Methane is a hydrogen-rich molecular material that is expected to dissociate at high pressure and temperature into an electrically conductive fluid.

We used static and dynamic coupling compression technique to generate icy planets core conditions in laboratory.

Methane was precompressed to ~0.4 GPa by DAC and then was shock compressed dynamically to pressures of more than 100 GPa.

We simultaneously measured pressure, density, temperature, and optical reflectivity for the highly compressed methane with velocity interferometers (VISAR) and optical pyrometer (SOP).

This work was performed under the joint research project of the ILE, Osaka University.

This work was partially supported by grants from the Core-to-Core Program of the JSPS, the Global COE Program CEDI of the MEXT, and the CREST of the JST.

Keywords: High-Power Laser, static and dynamic coupling compression, Methane, DAC

Physical properties of water and alcohol?water mixtures in the transition region between ionic fluid and plasma

Mika Kita^{1*}, Norimasa Ozaki¹, OKUCHI, Takuo², KIMURA, Tomoaki³, SANNO, Takayoshi², SAKAWA, Youichi², KODAMA, Ryosuke¹

¹Grad. school of Eng., Osaka Univ., ²Institute for Study of the Earth's Interior, Okayama Univ., ³Geodynamics Research Center, Ehime Univ., ⁴Institute of Laser Engineering, Osaka Univ.

Mixtures of water, methane, and ammonia at high pressures and temperatures are thought to be the major constituents of Ice Giants like Uranus and Neptune. Understanding of composition and formation of these planets relies on the existing equation-of-state (EOS) of the elements and compounds. However, these EOS and properties near phase boundaries (e.g. ionic fluid to plasma), where its physical and chemical properties are changing dramatically, have not known well. In order to understand planetary chemistry, laboratory measurements of the material properties are required in the transition regime.

We performed laser-shock compression experiments for liquid specimens to pressures of more than 100 GPa. We measured shock velocities, optical reflectivity, and shock temperature by using Velocity Interferometer System for Any Reflector (VISAR) and Streaked Optical Pyrometer (SOP). These experimental observables are compared between pure water and ethyl alcohol/water mixtures in the transition pressure-temperature regime. Optical reflectivity of the mixture is significantly higher than of water. We here discuss the effect of carbon ions on the mixture reflectivity.

This work was performed under the joint research project of the ILE, Osaka University. This work was partially supported by grants from the Core-to-Core Program of the JSPS, the Global COE Program CEDI of the MEXT, and the CREST of the JST.

Keywords: ice giants, water, mixture, phase transition, laser shock compression, equation of state

Orbital Evolution of Centaurs and their activity

Arika Higuchi^{1*}, Takeru Kobayashi¹, Shigeru Ida¹

¹Tokyo Institute of Technology

We have investigated the orbital evolution of Centaurs and their cometary activity.

According to the orbital integrations by many authors, Centaurs are thought to be objects that are transitioning between the Kuiper Belt region and the inner solar system. Due to the strong perturbations from giant planets, Centaurs have short dynamical lifetime of $\sim 10^7$ years: about two-thirds are ejected from the solar system and one third are injected into the inner region to be called Jupiter family comets (e.g., Volk&Malhotra 2008.) According to Jewitt (2009), 16 active Centaurs have been found. It is curious that some of such Centaurs show cometary activity. Their activity cannot be explained as an ordinal water sublimation of short-period comets since they are too cold for water sublimation to be effective and also too hot to keep CO ice. The alternative mechanism of their activity has been proposed and discussed in Jewitt (2009). Jewitt said that if Centaurs contain the amorphous ice that is porous and have enough space to keep CO gas, the CO outgassing occurs when the amorphous ice transforms into crystalline form. Observations of Centaurs support the hypotheses that the crystallization of amorphous ice (thermal process) is the trigger or driver of activity. But we have no idea how long the activity maintained. Guilbert (2012) calculated the 3-D thermal evolution of icy body due to the heat from the Sun in detail, including the seasonal variation. She found that the crystallization of amorphous ice is completed in 10^4 -5 years. However, Guilbert assumes circular orbits despite that the chaotic orbits and the short dynamical lifetime of Centaurs.

Now we try to combine the orbital evolution and thermal evolution. We calculate the orbital evolution of Centaurs and the crystalline fraction as functions of time. To calculate the crystalline fraction, we use equation (26) in Kouchi et.al. (1994) that gives the crystalline fraction of water ice under the temperature which varies with time. We calculate the temperature as a function of the heliocentric distance. We found that the crystallization timescale is much shorter than that of the propagation of the heat wave from the moment the object reaches a new surface thermal balance in the giant planets region, 10^4 -5 years, derived by Guilbert (2012). We also found that the orbital distribution obtained from observations is roughly well reproduced assuming Guilbert's timescale and our orbital integration. In the presentation, we will estimate and discuss the fraction of new Centaurs by comparing our results and the observations.

Keywords: Centaurs, orbital evolution, amorphous ice, cometary activity

Chemical composition diversity among impact-generated atmospheres on terrestrial planets: The effect of impact velocity

Hideharu Kuwahara^{1*}, Seiji Sugita¹

¹Complexity Sci. & Eng., Univ. of Tokyo

Prebiotic chemistry and climate conditions of early Earth and/or Mars would have been suitable for origin and evolution of life. The chemical composition of atmospheres during early evolution stages is important for understanding these factors.

Impact-generated atmospheres would occur on terrestrial planets immediately after their accretion and perhaps during the late heavy bombardment (LHB) period in the solar system. The approaches taken by previous studies on impact-generated atmospheres, however, may not have been accurate; they estimate the composition of impact-induced vapor with equilibrium calculation as a function of temperature under constant pressures [e.g., 1, 2]. This approach is appropriate if chemical reaction in impact-induced vapor is controlled by radiative cooling because radiative cooling decreases temperature while pressure is kept approximately constant. In reality, impact-induced vapor adiabatically expands; nevertheless such behaviors have not been considered. Entropy gain during the shock-compression phase controls the temperature-pressure pathway of the decompression phase. Thus, estimation of the initial entropy gain and subsequent quenching are the key for accurate estimation of the chemical composition of impact-generated atmospheres. The goal of this study is to model chemistry within adiabatically expanding impact-induced vapor, and investigate how sensitively impact-generated atmospheres depend on impact velocity.

Thermodynamically stable chemical compositions depend on temperature, pressure, and elemental compositions. Thus, constraints on these values are required for modeling chemical compositions of impact-generated terrestrial atmospheres. In this study, we assume CI chondrites as the impactor that mainly contributes volatiles to terrestrial planets during the heavy bombardment [e.g., 3]. To determine the temperature-pressure paths of adiabatically expanding vapor, we estimate the entropy gain during the shock-compression phase using the Hugoniot equation of state for silica [4]. Then, we calculate the major composition of a gas and condensed phase along isentropic lines within a range of pressures (0.01-10000 bars) and temperatures (500-2500 K). The model calculations are performed using a Gibbs free energy minimization code [5]. Elements included in our calculations are H, C, O, N, S, Mg, Al, Si, Fe. Elemental abundances used in our calculations are taken from [6].

Our calculation results show that the redox disproportionation of carbon occurs at low entropy states achieved by low-velocity impacts (<13km/s). For high-velocity impact (>17km/s), impact-induced vapor is rich in diatomic molecules, such as CO and H₂. For low-velocity impact-induced vapor (<13km/s), CH₄ becomes thermodynamically stable even at high quenching temperatures (>1000K). This is because the adiabatic curve for low entropy states undergoes higher pressures at a given temperature. High pressure is thermodynamically favorable for the formation of polyatomic molecules, such as CH₄ and NH₃; i.e., Le Chatelier's principle. These calculation results strongly suggest that the chemical compositions of impact-generated atmospheres among terrestrial planets may be different even if the composition of accreting material were same, suggesting that early Mars and early Earth may have possessed a CH₄-rich reducing atmosphere and a CO- and CO₂-rich more oxidizing atmosphere, respectively.

References: [1] Hashimoto G. L. et al. (2007) *JGR*, 112, E05010. [2] Schaefer L. and Fegley B. (2010) *Icarus*, 208, 438-448. [3] Alexander C. M. O' D. (2012) *Science*, 337, 721-723. [4] Kurosawa K. et al. (2012) *Am. Inst. of Phys.*, 855-858. [5] Gordon S. and McBride B. J. (1994) NASA Reference Publication 1311. [6] Wasson J. T. and Kallemeyn G. W. (1988) *Philos. Trans. R. Soc. London Ser. A*, 325, 535-544.

Keywords: Impact, Atmospheric composition, terrestrial planets

Impact experiments on a granular layer: an implication for crater scaling laws and the artificial Hayabusa 2 SCI crater

Sayaka Tsujido^{1*}, Ayako Suzuki², Masahiko Arakawa¹, Minami Yasui³

¹Graduate School of Science, Kobe University, ²Center for Planetary Science, ³Organization of Advanced Science and Technology, Kobe University

Introduction : Regolith formation and surface evolution on asteroid are caused by high velocity impacts of small bodies. The ejecta velocity distribution is one of the most important physical properties related to the crater formation and it is necessary to reconstruct the planetary accretion process among planetesimals. The surface of small bodies in the solar system has a various property on the porosity, strength and density. Therefore, the impact experiment on the target with the various properties is necessary to clarify the crater formation process applicable to the small bodies in the solar system. These results obtained from the target with the wide range of condition could help us to speculate the physical properties of the asteroid surface from the artificial impact crater made by Hayabusa 2-SCI. We would try to determine the surface strength and the porosity by means of the observation of the ejecta shape and the velocity distribution.

Experimental method: The cratering experiment was made by using a vertical type one-stage light gas gun (V-LGG) set at Kobe Univ. We newly developed a special sabot-stopper system to exclude the disturbance of accelerating gas from the growing ejecta curtain. We used 4 types of targets: that is, they are the 100micron-glass beads target (porosity 37.6%), the 500 micron-glass beads target (porosity 37.6%), the 1~3mm granular pearlite (porosity 96.7%) and the crushed pearlite with the size of a few 100 microns (porosity 84.9-88.4%). These granular materials were put into the stainless steel container with the diameter of 30cm and the depth of 11cm. The target container was set in a large chamber with the air pressure less than 10^3 Pa or 10^5 Pa. The material of the projectile that we used was an iron, a zirconia, an alumina, a glass, and a nylon, and it had a diameter of 3mm (2r) and was launched at the impact velocity (v_i) of 25 to 217m/s.

We made an impact experiment using an alumina sphere projectile on the 500-micron granular target and observed each glass bead by using a high speed digital video camera (nac memrecam HX-3) taken at 10^4 FPS. Then, we measured the ejection velocity and the initial position of each bead. We successfully obtained the relationship between the initial ejection velocity and the initial position for the bead ejecta. We also made the impact experiments on the 100-micron glass beads target and the pearlite target using various type of the projectile at a constant velocity of 100 and 200 m/s, and observed the crater size and the shape of ejecta curtain, especially for the ejecta angle.

Result: We found that the ejecting velocity of the glass bead for the 500-micron target decreased with increasing the distance from the impact point. The obtained empirical equation between the ejection velocity and the initial position is as follows, $v_e/v_i=0.66(x_0/r_0)^{-1.6}$, where v_e is an ejection velocity of glass beads, x_0 is the initial position of ejecting beads. The ejection angle of the beads is found to be almost a constant of 40 degree irrespective of the initial position. The crater size for the 100-micron target increased with the projectile density at the constant impact velocity and it was analyzed by using a crater scaling law to derive an empirical parameter characterizing the granular target. The relationship between the normalized crater size and the impact condition was written by $[R*(\rho_t/m)^{(1/3)}]/[(\rho_t/\rho_p)^{0.03}]=1.9*[gr/(v_i^2)]^{-0.17}$, where R is the radius of a final crater, ρ_t is the density of the target, ρ_p is the density of the projectile, m is the projectile mass, and g is the acceleration of gravity. From this obtained equation for the crater scaling law, we determined two key parameters of the coupling parameter ($C=r v_i^{\mu} \rho^{\nu}$): they are $\mu=0.40, \nu=0.36$. In the case of the crushed pearlite target, we found that the crater type changed from an incompressive type to a compressive type at the porosity from 83 to 88%.

Crater rays in impact experiments and numerical simulations

Toshihiko Kadono^{1*}, Ayako Suzuki², Koji Wada³, Satoru Yamamoto⁴, Masahiko Arakawa⁵, Seiji Sugita⁶, Akiko M. Nakamura⁵

¹University of Occupational and Environmental Health, ²Center of Planetary Science, ³Planetary Exploration Research Center, ⁴National Institute for Environmental Studies, ⁵Kobe University, ⁶University of Tokyo

Crater rays, which often adjoin the craters on the surfaces of the planets and satellites, appear also in laboratory impact experiments. Formation mechanism of such crater rays has been considered so far but not clear. Here, we carry out impact experiments with granular targets and observe the pattern formation in ejecta, taking consecutive images of ejecta by a high-speed camera, and final ray-patterns around craters. Also, we numerically investigate two-dimensional pattern formation process of granular materials using a discrete element method (DEM) simulation. Moreover, we analyze the crater rays on the surface of the Moon, using the satellite data of Kaguya.

Based these results, we find the characteristic features of the ray formation mechanism as,

1. Crater rays are not always straight in the radial direction; they complexly twine each other (intertwine).
2. Granular materials in the ejecta do not collide elastically each other during their flights.

We quantitatively compare the results of the experiments, numerical simulations, and satellite data analysis and investigate some scaling-laws about the relations between the ray patterns and the impact conditions such as the impactor size and velocity, the size of target granular particles, and gravity.

Keywords: crater ray

Effect of incident angle on crater dimensions with limestone targets

Ayako Suzuki^{1*}, Masato Kiuchi², Yasunari Komoto², Eri Matsumoto², Toshihiko Kadono³, Akiko Nakamura², Sunao Hasegawa⁴, Kosuke Kurosawa⁴, Masahiko Arakawa², Seiji Sugita⁵

¹CPS, Kobe Univ., ²Kobe Univ., ³Univ. Occupational and Environmental Health, ⁴ISAS / JAXA, ⁵Univ. Tokyo

Impact craters are common on the surface of solid bodies in our Solar system, and the majority of them are formed in oblique impacts. The effects of incident angle on impact cratering are important to derive scaling laws of impact craters and to understand the formation of secondary craters. However, there are not much experimental data of oblique impacts, especially in the strength regime. Recently, high-resolution images of the surface of planets and small-bodies allow us to see small craters in meters (e.g. McEwen et al., 2007). There are many terrestrial craters in the strength regime, such as the Carancas crater (e.g., Tancredi et al. 2009) and the Kamil crater (Folco et al. 2011). In this study, we performed impact experiments into sedimentary rock varying incident angle, to examine the effect of the angle on the crater dimensions.

Two-stage light gas gun placed in ISAS/JAXA was used. The projectiles were nylon spheres of 7 mm in diameter. The targets were blocks of limestone with 15 cm cube. The tensile strength, bulk density, and porosity of the limestone are 4.6 MPa, 2.24 g/cm³, and ~17%, respectively (Suzuki et al. 2012). The impact velocity is ~2.5 km/s, and the incident angle (theta; measured from the target surface) is varied as 5, 10, 20, 30, 45, 90° (vertical impact). The impacts are recorded by a high-speed digital video camera. After each shot, we measured the length (the maximum dimension of the crater along the projectile trajectory) and width (the maximum dimension perpendicular to the trajectory) with a digital caliper. We also made 'a digital topographic data' of the crater by means of a digital microscope (KEYENCE, VHX-1000), then obtained the crater volume and depth.

There is a pit in the center of the crater at the vertical impact (theta=90°), while no noticeable pits are observed in craters of theta < 45°. The ratios of lengths, widths, depths, and volumes against the values of vertical impacts are proportional to (sin theta)^{0.54 ± 0.01}, (sin theta)^{0.49 ± 0.01}, (sin theta)^{0.66 ± 0.02}, (sin theta)^{1.61 ± 0.09}, respectively. The power of the volume ratio (1.61 ± 0.09) is similar to those obtained by aluminum impacts into granite (Gault and Wedekind 1978; 1.80 ± 0.16). In the strength regime, it is known that the crater volumes are proportional to the impact energy (namely, to the square of the impact velocity). Our results are consistent with the concept that crater-scaling relations can adequately accommodate the impact-angle effects by using only the vertical velocity component (Gault and Wedekind 1978; Chapman and Mckinnon 1986).

The ratio between the length and width is constant of 1.11 ± 0.11 over the range of the incident angle from 90° to 5°, while the critical angle where the ratio deviate from unity is ~15° (Gault and Wedekind 1978) and ~5° (Burchell and Whitehorn 2003). One reason for this may be that the nylon projectile is easy to break and the top part of the projectile does not shear off (so-called 'impact decapitation' (e.g., Burchell and Whitehorn, 2003)). Without impact decapitation, the length of the crater decreases when theta decreases, in the same manner as the width decreases. However, the crater of 5° in incident angle has a raised part in the downstream side, suggesting it would be a spall fragment when it's tore off. In the strength regime, spall fragments play a big role in shaping craters. We need a number of shots to minimize the effects of spall fragments.

Averaged diameter is defined as the average of length and width of the crater. The crater depth normalized by the averaged diameter is constant of 0.16 ± 0.01 in the range of theta from 20° to 90°. The normalized depth at theta = 5° and 10° is smaller than the value. This trend is due to depths becoming small faster than lengths and widths, and would be because the density of the nylon projectile is about a half of that of limestone target and the projectile is difficult to penetrate the target.

Effect of surface layering on the apparent thermal inertia

akari yoshida^{1*}, Takenori Toyota¹, Kei Kurita¹

¹Earthquake Research Institute, The University of Tokyo

Thermal inertia is a key property controlling diurnal temperature variation at the surface of planets. It is defined as a function of thermal conductivity, heat capacity, and density, all of which depend primarily on the physical structure of the surface layer. Thermal inertia of Mars has been derived from Viking, Mars Global Surveyor and Mars Odyssey data. It tells us a structure of the surface layer. For example, low thermal inertia indicates extensive dust deposits and higher thermal inertia suggests combination of particle size, rock abundance and induration of soils.

An extremely low thermal inertia values such as 5-60 tiu and 24-60 tiu have been reported in the equatorial and middle latitudes from these observations. Since the thermal conductivity is the most sensitive to the particle size under martian atmospheric pressure, such a low thermal inertia indicates small grain size as low as 10 micron. But, these particles can be easily blown away by a strong wind on Mars and it is difficult for them to form a uniform layer on the structure. In this presentation we consider the possibility that a layered structure yields apparent low thermal inertia.

To demonstrate possible effect of the layering we conducted laboratory experiments. We utilized the structure having an acrylic plate on top of a polystyrene form block or vesiculated particle layer. They are heated periodically by an infrared lamp from above. Using the infrared thermometer and thermocouples, we measured the temperature at the surface, bottom of the acrylic plate and inside the lower Polystyrene form and the granular layer.

Thermal relaxation time of this layered systems is the most fundamental factor here, which represents the time that the amplitude of temperature inside the material becomes 1/e compared with the surface.

We estimated the thermal inertia from experimental data. It is found that the thermal inertia is lower than the value calculated from the physical properties when the given period is longer than the thermal relaxation time of the surface layer. It is because the material behaves infinite body when the period is shorter than the thermal relaxation time.

On the other hand it behaves as a finite body if the period is longer than the relaxation time. In this situation the temperature at the bottom of the surface acrylic plate becomes high because of lower thermal conductivity of the lower layer. This means the thermal gradient becomes lower and the heat flux to the interior seems small, which results in apparently low thermal inertia

In our experiments we can demonstrate a simple layered structure; a thin layer having higher thermal conductivity on top of a layer with low thermal conductivity can produce apparently low thermal inertia. In the martian remote sensing diurnal temperature variation is used to infer the thermal inertia, which measures the value of the surface within the thermal penetration depth of several to 10 cm. If the layered structure exists in this range having lower conductivity of the lower layer.

We discuss several geological processes to produce layered structure on Mars.

Keywords: thermal inertia, geological structure, thermal relaxation time

Effects of the temperature dependences and surface roughness of the asteroid 1999JU3 on the surface temperature mapping

Jun Takita^{1*}, Satoshi Tanaka², Hiroki Senshu³, Tatsuaki Okada²

¹Graduate school of science, Tokyo university, ²Institute of Space and Astronautical Science, JAXA, ³Planetary Exploration Research Center, Chiba Institute of Technology

The observational program with thermal infrared imager to detect its target asteroid 1999JU3 and the strategies to estimate the surface physical state with obtained data are now under constructed in Hayabusa 2 mission. It is necessary to clear and understand the mechanism to realize the observed space-resolved data of surface temperature. We consider the temperature dependence of surface material plays important role in surface temperature of airless small bodies, especially NEA asteroids which maximum and minimum temperature differ significantly. In addition to this, we are now investigating the effect of the surface roughness on surface temperature distribution of asteroids and comets. The beaming parameter which has close relationship with surface roughness is necessary for the explaining the ground based spatially-none-resolved surface brightness and temperature of asteroids. Recent DEEP-IMPACT or EPOXI missions have revealed that the shape model alone could not be enough to reproduce the observed surface temperature distributions but it would be possible with the help of the effect of surface roughness in some appropriate ways. The surface roughness would also generate the interactive heating effect through radiative energy exchanges between its and adjacent surfaces.

We took six orbital elements into account to calculate the planetary position of the asteroid as well as the orientation of the spin axis so as to simulate the distance from the sun and the incident angle of solar energy into the surface. The shape of the numerical model is set to be spherical and subject to one dimensional heat conduction equation in none steady state. We have made the temperature mapping of the target asteroid to use this model. The distribution of thermal properties of heat conduction medium is constant toward inner direction, which has temperature dependencies except for the density. We applied the experimental result of temperature dependencies of lunar samples to this model. The numerical calculation showed that the difference of surface maximum temperature in one rotation near perihelion was about 10K between temperature dependent and none-dependent models. Thus we thought this effect would not be negligible to derive the thermal inertia of the asteroid with TIR instrument. We have now been performing the estimation of the effect of surface roughness on the surface temperature to construct some simple models. We will present the result of this effect on this meeting.

It is important to distinguish the geometric effects from the thermo physical effects to estimate the physical state of the planetary surface. This is not only indispensable with the determination of sampling rate of TIR thermal images but also practical in SCI impact experiments in terms of finding the locations of impacting center and the smashed debris.

Keywords: Hayabusa2, thermal infrared imager, thermal inertia, temperature dependence, roughness, equation of heat conduction

Thermal conductivity measurements of sintered powder under vacuum condition

Shoko Tsuda^{1*}, Kazunori Ogawa¹, Naoya Sakatani¹, Yu-ichi Iijima¹, Rie Honda², Satoshi Tanaka¹

¹Institute of Space and Astronautical Science, ²Kochi University

In the planetary formation process, powder like dusts would have formed into planetesimals that have grown into proto-planets or asteroids through collisions between each other. Although efficiency of collisional accretion depends on physical properties (such as density and strength), their change due to thermal metamorphism has not been fully understood. Some planetesimals might have served as parent bodies of meteorites, and evidence of their thermal metamorphisms could give us information of size and formation time of the planetesimals. Therefore, it is important to investigate their thermal evolution and resultant change in the physical properties.

Thermal conductivity of the planetesimal constituents is one of the important parameters for examination of the thermal evolution. While the thermal conductivity of typical rocks is about 1 W/mK, that of powder is in the order of 0.001 W/mK under vacuum, which is lower than the value of rocks by three orders of magnitude. Because of thermal insulation by the powdered materials, even small planetesimals with the radius as small as 10km might have experienced temperature more than 1000 K (Ogawa, 2013), so that sinter bonding might have formed between powder particles that could have caused a significant change of the thermal conductivity.

Henke et al. (2012) calculated the thermal evolution of primitive porous planetesimals consisted of powdered materials as a model of parent bodies of chondrites. They assumed that sintering occurred as the internal temperature increased, which process made planetesimals thermal conductivity higher by one to two orders of magnitude. Measured data of thermal conductivity of some kind of powders under vacuum is available (e.g. Sakatani et al., 2012), but there are few reports, in which the thermal conductivity of sintered material is measured. In their study, they used thermal conductivity derived as a function of porosity based on the measured value of silicate powder and chondrites.

However, based on our measurements of the thermal conductivity of glass beads (Sakatani et al., 2012), a positive correlation between the thermal conductivity and the pressure (thus, the inter-particle contact area) was observed. Therefore, the thermal conductivity should be re-examined as a function of the contact area instead of porosity.

In this study, we aim at investigating thermal conductivity of the sintered materials under vacuum condition, in order to provide constraints on the thermal conductivity of the sintered materials in planetesimals. Glass beads of several particle sizes were used as pre-sintered powder samples.

For sample preparation, we examined neck radius variation due to the heating temperature and the heating duration using a theoretical expression (Sirono, 1999; Poppe, 2003). The results indicated that, in order to make the neck radius 10 times larger than that is formed by heating for 0.1 hours, increasing heating time to 1000 hours are equivalent with increasing heating temperature by 100 K. Thus we adopted change the heating temperature instead of heating duration to control the sintering contact area.

Currently we are planning to measure the thermal conductivity of sintered samples by so-called line heat source method. Two methods are considered for installation of a heat system in the samples: (1) putting the system in the glass beads and then heating both samples and the system to induce sintering of glass beads and (2) putting the system between two separate sintered samples created under the same condition. In the former case, heating during sintering may induce the change of electric resistance of the heating wire by oxidation and melting of a resin used between the wire and the thermocouple. The latter case is free from these problems, thus we adopted the latter method for installation of the line heat source system. We present detailed explanation of the measuring method and results of these experiments in the presentation.

Keywords: sintering, powdered materials, thermal conductivity

Early thermal evolution of planetesimals considering low thermal conductivity of powdered materials

Maho Ogawa¹, Naoya Sakatani^{1*}, Yu-ichi Iijima¹, Kazunori Ogawa¹, Shoko Tsuda¹, Rie Honda², Masahiko Hayakawa¹

¹Institute of Space and Astronautical Science, ²Kochi University

Dust materials in protoplanetary disk accumulated into planetesimals. Protoplanets and asteroids have been considered to be formed by the collisions between the planetesimals. Efficiency of the collisional growth depends on physical properties and internal structure of the bodies. Therefore, it is important to consider the evolution of the physical properties and internal structure of the planetesimals due to thermal metamorphism. In previous studies, the thermal evolution of meteorites parent bodies were calculated in combination with metamorphic temperature or cooling rate estimated from the meteoritic analysis. However, most of these studies used the physical properties, such as thermal conductivity and density, of the meteorites as initial parameters of the parent body. Since the planetesimals accumulated from the dusts are considered to be porous bodies consisted of powdered materials, the above assumption would be improper. The initial properties of the planetesimals are important parameters controlling the thermal evolution and the resultant change of the internal structure. Among these initial properties, we focused on the thermal conductivity.

It is known that the powdered materials have low thermal conductivity compared with rocks having the same composition. Especially under vacuum environment, silicate powders have extremely low thermal conductivity about 0.001 W/mK. Therefore, if assuming the porous body consisted of powdered materials as the initial structure of the planetesimal, the subsequent thermal evolution would be different significantly from the previous models that assumed the physical properties of the meteorites. In this study, we aimed at investigating the effect of the powdered materials of low thermal conductivity on the thermal evolution of the planetesimals.

We numerically solved the equation of one-dimensional and spherically symmetric heat conduction, with the thermal conductivity, porosity, and formation time and size of the planetesimal as variable parameters. For the thermal conductivity of the powdered materials, which is the most interesting parameter in this study, we used experimental values we measured for glass beads (porosity of 40%) under vacuum. Since the thermal conductivity of the powdered materials depends on the cube of the temperature, it varies significantly during the thermal evolution. The temperature dependence was also included in our model.

We found that even planetesimals as small as 10 km in radius experience the significant heating above 2000 K at the center (see figure). Previously, it has been considered that the radius of the planetesimal about 100 km is required in order to heat up sufficiently to form the thermally metamorphic meteorites. Our calculation indicates that the planetesimals smaller than 10 km can serve as the parent bodies of chondritic and/or differentiated meteorites.

When comparing the temperature evolution between the models including and excluding the temperature dependence of the conductivity, the former had lower peak temperature by about 500 K than latter. While the temperature was maintained around the peak temperature for more than 100 m.y. for the latter case, for the former case the temperature dropped to a half of the peak temperature after 20 m.y. Therefore, the temperature dependence of the thermal conductivity of the powdered materials should be included in the model calculation.

When the temperature increases, the powdered materials will be sintered at a certain temperature. Because the thermal conductivity of the sintered materials will be higher than the not-sintered powdered materials, the sintering affects the subsequent thermal evolution. Furthermore, the change of the physical properties after the sintering would be important for the collisional growth between the planetesimals. In this presentation, we will also present the calculation results that include the effect of the sintering.

Keywords: powdered materials, planetesimal, thermal evolution

PPS21-P14

Room:Convention Hall

Time:May 20 18:15-19:30

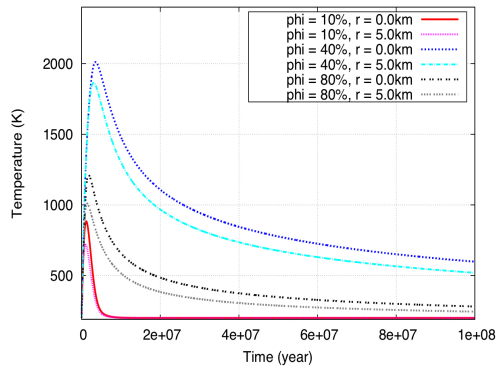


Figure: Thermal evolution of planetesimals of 10 km radius formed at 2 m.y. after CAI formation. "phi" and "r" in the legend refer to the porosity and distance from the center, respectively.

Experimental study on the impact strength of planetary bodies damaged by multiple collision

Ryo Hayama¹, Masahiko Arakawa^{1*}, Minami Yasui², Yuri Shimaki³

¹Graduate School of Science, Kobe University, ²Organization of Advanced Science and Technology, Kobe University, ³Graduate School of Environmental Studies, Nagoya University

High velocity collisional disruption of small icy bodies is one of the most important physical process related to the formation of the debris disk and the collisional growth of planetesimals in the outer solar nebula. Therefore, there are a lot of studies on the collisional disruption of icy bodies such as polycrystalline ice and snow systematically. As a result, the impact strength of polycrystalline ice was obtained to be 90 J/kg, and the snow was found to change the impact strength with the porosity. While in the case of the collisions among the real small bodies, the bodies could be sometimes collided at many times before they were disrupted. We definitely observe so many craters on the surfaces of icy bodies and the large crater that is more than a half of the size is also observed in many icy bodies. Thus, we should consider the effect of these pre-impact damages in the icy bodies when we apply our laboratory results to the real collisions in the solar system. Because these pre-impacted bodies could be weaker than the intact bodies. Therefore, we studied the effect of pre-impact damage on the impact strength of polycrystalline ice systematically, and the effects of the pre-impact time and the each impact energy on the impact strength was determined quantitatively.

Impact experiments were made by using a vertical gas gun set in a large cold room which room temperature was -15 degree or -10 degree. The ice target was a cube with the size from 3 to 10 cm ($M_t=100 - 3000$ g) and the projectile was a icy cylinder with the size of 1.5cm or 1cm ($m_p=1.5$ g or 0.2g). The impact velocity was from 100 to 480 m/s, and the projectile was collided on the different surface of the cube target or the same surface for the multiple impact experiment. We also change the energy density given to the target for each impact. After the impact, the target was recovered to measure the weight of each fragment. When the target was not disrupted severely, the elastic velocity through the recovered target was measured at 3 different positions. We also measured the static indentation strength of the recovered target, so the target was sliced into 3 plates and there plates were slowly pushed by an indenter. The elastic wave velocity of each plate was measured before the indentation test. Then, we tried to obtain the relationship between the elastic wave velocity and the indentation strength.

In the case of the impact at the different surface of the cube target, we found that the sum of the energy density for each impact (Q_{sum}) was a good parameter to describe the impact strength because the relationship between Q_{sum} and the largest fragment mass consists each other irrespective of the impact time and they are consistent with the result of the intact ice disrupted at once. In the case of the impact at the same surface, the Q_{sum} was apparently larger than that was necessary for the impact at the different surface. This difference of the impact strength depending on the impact surface could be caused by the difference of the internal crack density and the distribution. Then, we studied the relationship between the elastic wave velocity and the indentation strength, and we obtained the following empirical equation, $Y/Y_0=1-1.34 dV/V^{0.78}$. We applied this equation to the scaling parameter P_I proposed by Mizutani et al. (1990) and studied the relationship between P_I and the largest fragment mass. Thus, we found that all the data merged on one line and the empirical relationship was obtained to be $m_l/M_t=0.0413P_I^{-4.82}$. So, the effect of the pre-impact damage by multiple impacts is found to be quantified by the elastic velocity. This enable us to estimate the impact strength of the real small icy bodies by the measurement of the elastic wave velocity of these interiors.

Keywords: icy planetesimals, impact disruption, crack, sound velocity, mechanical strength, scaling law

Dynamic compaction experiments of snow: Implications for low-velocity impact compaction of icy pre-planetesimals

Minami Yasui^{1*}, Kana Sakamoto², Masahiko Arakawa³

¹Organization of Advanced Science and Technology, Kobe University, ²Faculty of Science, Kobe University, ³Graduate School of Science, Kobe University

Introduction: In the standard solar model, planetesimals could form by gravitational instability in the dust layer of a proto-planetary disk. However, there is a significant problem that planetesimal could not grow because of dust settling disturbance by turbulent flow in the disk. We focused on a pre-planetesimal, which is a body with the diameter of cm to several hundreds meters. Recently, some researchers suggest that planetesimals could form by impact coagulation of pre-planetesimals. However, there are also some problems, such as catastrophic disruption. Some researchers studied the formation processes of pre-planetesimals by numerical simulations. Geretschauser et al. (2011) proposed the impact model of porous silicate-dust aggregates, and found seven impact regimes (compaction, disruption, and adhesion) depending impact velocity and size ratio of impactor and target, and the compaction degree was different with regime. However, this model did not include compaction curves measured in laboratory experiments. In this study, we conducted low-velocity impact experiments for high porous snow simulating icy pre-planetesimals, and studied the impact compaction conditions. We measured the density profile changing with depth, compaction area size, and stress, and obtained the empirical equations related to density distribution and compaction area.

Experimental methods: We did impact experiments in the cold room at -10 degree C in ILTS, Hokkaido University. The projectile was a stainless cylinder with the diameter of 25 mm, the height of 40 mm, and the mass of 149 g. On the lower, a PVC disk with the diameter of 26 mm was set due to suppress the ejecta. The projectile was accelerated by free fall, and the drop distance changed from 50 to 900 mm. The impact velocities were 0.7 to 3.5 m/s. The target was prepared by packing ice grains into the acrylic tube with the diameter of 26 mm. The porosities were 70, 80, and 90 %. Ice grains were made by spraying water into LN₂, and then the ice grains were sieved to sort grains from 50 to 500 micron-m. The target has the length of 100 mm, and the blue ice grains were put into the target every 20 mm from the bottom due to measure the density changing with depth. The blue ice grains were produced by spraying blue water into LN₂. The impact compaction of the target was observed by a high-speed digital camera. The shutter speed was set to be 20 and 50 micron-s, and the frame rate was set to be 3000 and 5000 fps. The acceleration sensor was set on the upper surface of projectile to measure the stress. The voltage measured by acceleration sensor was recorded by oscilloscope and data logger. The sampling number of data logger was set from 2.5×10^5 to 10^6 and the sampling interval was set to be 20 micron-s.

Results: We analyzed the stress by using the data of acceleration sensor and high-speed camera images. The maximum stress, s_{max} , which is defined to be a maximum stress on the stress profile, was 20-100 Pa for 70 % snow, and 15-50 Pa for 80 % snow, and that of 70 % snow was 1.3-2 times larger than that of 80 % snow. Additionally, the s_{max} increased with the impact velocity in both targets. The stress obtained from the data of acceleration sensor corresponded to that for high-speed camera images. Furthermore, the yield strength, Y , calculated by Kinoshita method and these obtained stresses were almost same. Next, we compared the final density of uppermost layer of target, r_1 , and the s_{max} to study the density profile. As a result, the r_1 increased with the s_{max} , the relationships between r_1 and s_{max} were expressed as $r_1 = 1.7 \times 10^2 s_{max}^{0.2}$ for 70 % snow and $r_1 = 1.2 \times 10^2 s_{max}^{0.3}$ for 80 % snow, respectively. Finally, we calculated the bulk modulus, K , by using the relationship between the yield strength, Y , and the average density of target, r_{ave} , and the K was 1.8 MPa for 70 % snow and 0.2 MPa for 80 % snow, respectively.

Keywords: icy pre-planetesimal, impact compaction, low-velocity impact experiment, density profile, compaction area, bulk modulus

Evolution of planets with oceans within the Water World Regime around a main sequence star

Satoshi Fukushima^{1*}, Shintaro Kadoya¹, Eiichi Tajika²

¹Department of Earth and Planetary Science, The University of Tokyo, ²Department of Complexity Science and Engineering, The University of Tokyo

The Habitable Zone (HZ) around a main sequence star is the orbital condition in which planets could have liquid water on their surface, although greenhouse effect of the atmospheres due to some greenhouse gasses (e.g., CO₂) is generally required. On the other hand, we propose here the Water World Regime (WWR) which is the orbital condition for the planets to have liquid water even if the planetary atmospheres do not have any greenhouse gasses except water vapor. The WWR is therefore much narrower condition than the HZ, estimated to be an annual mean insolation from 1.07 to 1.41 S₀ (where S₀ is the solar constant for the present Earth). Most of the WWR condition is, however, under the moist greenhouse condition in which water should escape to space during the planetary evolution (e.g., Kasting, 1988). The time scale of water loss should therefore be discussed for the planets with different amount of H₂O and XUV from the central stars.

We estimated life time of oceans on the planets orbiting within WWR by assuming water loss due to hydrogen escape by diffusion-limited (Hunten, 1973 ; Walker, 1977), and energy-limited water loss mechanisms (Watson et al., 1981), with considering stellar luminosity evolution (Gough, 1981 ; Iben, 1967), and stellar EUV evolution (Lammer et al., 2009).

We will show that the life time of oceans may be longer than that considered generally. For example, if the Earth is orbiting within the WWR around a M-type star and has liquid water of 5 times the amount of ocean today, liquid water may be able to exist for 10 billion years.

Keywords: Extrasolar planet

Climate evolution of extrasolar terrestrial planets with water and carbonate-silicate geochemical cycle

Shintaro Kadoya^{1*}, Eiichi Tajika²

¹The University of Tokyo, ²The University of Tokyo

The surface environment of a habitable planet has been constrained in terms of orbital semi-major axis and an effective solar flux, focusing on the existence of liquid water, that is, the habitable zone (HZ) around main sequence stars (e.g., Kasting et al., 1993). It has been also pointed out that the carbonate-silicate geochemical cycle would be essential for maintaining the climate of a habitable planet (e.g., Tajika, 2003). However, the whole picture of evolution of climate of planets with carbonate-silicate geochemical cycle has not been known.

In this study, we investigate the climate evolution of an Earth-like planet (actually, the Earth itself) around a G-type star (= Sun). Steady states of climate of Earth-like planets are estimated systematically with a simple climate model coupled with a carbonate-silicate geochemical cycle model. We classified climates of Earth-like planets within the HZ into three modes, in terms of stabilizing mechanism. Then, the climate evolution is estimated based on the steady state solutions of the climate with models of the stellar evolution and the thermal evolution of planetary interiors. The results indicate that, on an Earth-like planet (the size of the Earth) orbiting around a G-Type star, climate depends on the thermal history of the planet in the early stages of its lifetime, and then depends on the stellar evolution. The climate evolutions are also estimated for the different mass both for stars and planets.

Keywords: Extrasolar planetary system, Habitable zone, Habitable planet, Carbonate-silicate geochemical cycle, EBM

Local N-body Simulation for Accretion of Particles onto Moonlets in Saturn's Rings

Yuki Yasui^{1*}, Keiji Ohtsuki², Hiroshi Daisaka³

¹Dept. Earth Planet. Sci., Kobe Univ., ²Dept. Earth Planet. Sci., Kobe Univ./CPS, ³Hitotsubashi Univ.

Gravitational accretion of particles in circumplanetary disks is an important issue related to the origin of ring-satellite systems of giant planets in the Solar System. Observations by the Cassini spacecraft indicate that the small satellites within the orbit of Pandora orbiting just outside Saturn's F ring were formed by accretion of small porous ring particles. N-body simulations demonstrated that a Hill sphere-filling body is produced by accretion of small porous particles onto a larger dense core. Propeller-shaped structures, which are produced by unseen embedded moonlets, have also been found in Cassini images of Saturn's A ring. Some of these moonlets may have formed by accretion of small low-density ring particles onto larger dense fragments. Thus, accretion in the rings may also be related to the origin of these embedded moonlets.

The criteria for gravitational accretion of particles in the Roche zone was derived based on the Hill approximation in the three-body problem. The criteria, which we call the "three-body capture criteria", state that colliding particles can become gravitationally bound if they are within their mutual Hill radius and E becomes negative value after inelastic collisions, where E is the sum of the relative kinetic energy and tidal potential energy of colliding particles. Furthermore, using the criteria, capture probability for collisions between ring particles was obtained by three-body orbital integration. However, many-body effects, which are not included in three-body calculations, are expected to become important as accretion of particles proceeds and aggregates are formed.

In our local N-body simulation, a moonlet is fixed at the center of the rectangular simulation cell. For each time step, particles not yet perturbed by the moonlet are added to the cell from the azimuthal boundaries. Particles leaving the simulation cell through the azimuthal boundaries are removed from the cell, but we retain the periodic boundary condition in the radial direction. In order to examine the accretion process and timescale for the growth of the moonlet in detail, we count the number of particles that form an aggregate by two different methods. First, we use the above three-body capture criteria for the moonlet and each of the colliding particles, and examine if a particle is gravitationally bound within the Hill sphere of the moonlet. However, in this method, the self-gravity of the particles accreted by the moonlet is neglected, and we underestimate the number of particles in the aggregate, because the number of particles accreted onto the moonlet increases with time. Second, in order to correct the above problem, we count the number of particles touching the aggregate as a member of the aggregate; we call this the "aggregate criterion".

Using the aggregate criterion, we calculate the accretion rate as a function of time, for calculations at the distance from Saturn that corresponds to $R_p=0.7$, where R_p is the ratio of the sum of radii of colliding particles to the Hill sphere radius. The accretion rate obtained by the N-body simulation agrees well with that obtained by the three-body calculation at the initial stage of accretion. As accretion of particles proceeds, the result of N-body simulation is slightly larger than the three-body results, because a significant number of particles have accreted onto the moonlet by this time, and the collision cross section of the aggregate is increased. After that, the aggregate reaches a quasi-steady state with a nearly constant number of constituent particles. Then, the aggregate repeats accretion and releasing of particles again and again. We also calculate the number of particles in the aggregate using the two different methods. We find that the three-body capture criteria underestimate the number of particles in the aggregate. The result obtained from the aggregate criterion also shows recurrent accretion and release of particles in the quasi-steady state.

Keywords: accretion, moonlet, Saturn's rings, N-body simulation

Inelastic Collisions between Icy Bodies: Dependence on Impact Velocity and Its Fluctuations

Koji Uenishi^{1*}, YANO, Ryosuke², Tatsuya Yoshida¹, Keisho Yamagami¹, SUZUKI, Kojiro²

¹Dept Aero/Astronautics, Univ Tokyo, ²Dept Adv Energy, Univ Tokyo

In a ring system, energy loss during collisions of particles may play a crucial role in determining not only the mean free path between collisions but also the physical characteristics of the ring (e.g., kinematic viscosity, spreading rate, thickness, shape) and the rate of cooling in the system. The coefficient of restitution is a key parameter for evaluating such energy loss during collisions (Dilley and Crawford, 1996). Icy particles are commonly found in the rings of Saturn, and due to their closeness to our living environment, their coefficient of restitution has been intensively studied. Earlier works on collisions of icy bodies normally suggest that the restitution coefficient strongly depends on the impact velocity. More recent approach to the problems of energy loss and cooling in a ring system includes the concepts developed in the theory of granular flow, but due to the lack of precise information about the velocity dependence of the restitution coefficient, it is often assumed that the coefficient is constant (velocity-independent) in granular flow-based analyses of inelastic collisions. Here, in order to better understand the physical characteristics of ice as a granular material and gain more quantitative information about the effect of impact velocity on the collisions of icy bodies, first, we experimentally monitor the mechanical behavior of an ice sphere impinging upon a plate of ice (235 mm x 320 mm x 60 mm) with a digital high-speed video camera system introduced in our laboratory. The diameter of an ice sphere is either 25 mm or 50 mm, and each sphere is kept in a freezer at a temperature of -10 degrees Celsius for more than 30 hours before every experiment starts. We intend to obtain the variation of the normal restitution coefficient for the free fall of spheres with 17 different falling distances between 40 and 450 mm. For that purpose, we take full-color digital photographs at a frame rate of 7,000 frames per second and record the collision process: From the photographs, we can calculate the velocities of an ice sphere just before and after the collision and with these velocities we may evaluate the normal restitution coefficient. We perform our preliminary series of experiments on collisions of ice spheres at least 10 times for each sphere size and falling distance at room temperature of 21 degrees Celsius. The range of falling distance mentioned above gives an impact velocity of 60-370 cm/s for 25 mm diameter spheres and 90-380 cm/s for 50 mm diameter ones. Care is taken not to induce any rotation and fracture of the ice spheres during the collision process. We also observe the roughness of the sphere surfaces as well as the fluctuations of the obtained coefficient for each sphere size and impact velocity. Then, based on the ED (Event-Driven) method, we perform numerical simulations of the cooling process during collisions of 3,000 ice spheres that are initially located randomly in a two-dimensional square. In the simulations, the experimentally obtained velocity-dependent restitution coefficient and its fluctuations are taken into account for the inelastic collisions between ice spheres. The results show the final temperature is about 4 % lower than that obtained without considering the fluctuations of the velocity dependence of the coefficient.

Keywords: ring system, icy bodies, inelastic collision, coefficient of restitution, cooling process, granular flow

Development of a simplified 3D shape measurement system for micro spherical object: application to chondrules

Keisuke Nishida^{1*}, Ayaka Tsuda¹, Eiichi Takahashi¹, Taishi Nakamoto¹

¹Earth and Planetary Sciences, Tokyo Institute of Technology

We developed a simplified system to measure the 3D shape of micro spherical object such as chondrules. This system consists of macro photography lens, consumer digital camera, and automatic mechanical stages and has a capacity to shoot pictures at up to 0.85 um/pixel. The camera and stages are automatically controlled by PC. Photographic images of a sample were obtained every 2 degrees up to 180 degrees in backlight to enhance the contrast between sample and environment for ease of binarization in image processing. The images were binarized and extracted coordinates of the outline of the sample in every degree to construct the 3D shape of the sample by our own software. The 3D shape can be exported as STL file, which is very common file format for 3DCAD and CG software.

In this study, we report the measuring results of 3D shape of chondrules separated from Allende CV3 chondrite (Tsuda et al, JPGU 2013).

Keywords: 3D shape, chondrule, Allende CV3 chondrite, spherical micro object

Chondrule Formation by Planetesimal Bow Shocks

Fumika Yamazaki^{1*}, Taishi Nakamoto¹

¹Tokyo Institute of Technology

Chondrules are mm-sized silicate particles included in most meteorites. Though it is known from experiments and observations that they experienced flash heating and melting in the solar nebula, the heating mechanism is still unknown. To comprehend chondrule formation may lead to understanding the environment in the solar nebula and the solar system formation.

One of the ideas for heating mechanism is the shock wave heating model. The model explains that, when the precursor dust grains run into the shock, they experience the gas drag heating, and dust temperature exceeds the melting point (e.g., Hood & Horanyi, 1991; Iida et al., 2001). In this study, we conduct detailed examination of dust heating by planetesimal bow shocks, which are the shocks occurring around eccentric planetesimals.

We carry out the calculation of 2-D grain trajectory and thermal history in the flow around the planetesimal taking account of melting and evaporation of the grains, which was not included in 2-D calculations of previous studies about planetesimal bow shock model (e.g., Nakajima, 2010, master thesis; Morris et al., 2012). Moreover, for detailed examination, we use the gas flow which is obtained by 2-D hydrodynamics simulations with H₂ dissociation and recombination as the background of grain motion.

Our results show that the grains avoid collision with the planetesimal thanks to the evaporation in some cases, and it affects the chondrule formation efficiency and the resultant size of heated grains. Using our calculations, the size distribution of chondrules and compound chondrule formation could be investigated and compared with the observations. We also show the chondrule formation condition by calculations with various nebula gas density and relative velocity of planetesimal to gas. Our results support the expectation that the solar nebula was more massive than MMSN model and that chondrules were formed in inner region of 3AU from the Sun.

Keywords: chondrule, bow shock, planetesimal, solar system formation, hydrodynamics simulations

Dust accumulation caused by thermal interaction between gas and dust in gas shock regions

Keisuke Watanabe^{1*}, Taishi Nakamoto¹

¹Tokyo institute of technology

Meteorites are important clues to investigate the environment of the early solar system. Chondrules are 0.1mm ? 1mm sized spherical igneous structure which are abundantly found in chondritic meteorites. Chondrule precursor dust grains once experienced melting caused by certain heating event, then recrystallized and formed their spherical form. Experimental constrains suggest that heating event was intense, heating duration is of the order of a few minutes and these events continued intermittently about three million years. This heating process was surely dominant in the early solar system but details are still unknown.

The most promising heating source for chondrule formation is gas shock wave heating in the protoplanetary disk. Previous works showed that gas shock waves can heat up the precursor dust grain temperature above melting point due to frictional heating. Iida et al. (2001) also showed that the gas temperature is higher than the dust temperature when the dust stops in the gas and its temperature attains maximum. In such a situation, the dust acts as coolant for the gas.

The gas in a relatively high dust density region is preferentially subjected to cooling by the dust. This preferential cooling makes the gas pressure minimum. Then the gas flows into the region because of the gas pressure gradient. This flow drags the dust into the high dust density region and it leads to further dust density enhancement. This one way thermal instability process may cause dust accumulation. Previous works concerning the gas shock wave heating model did not consider this process at all.

Here we investigate the possibility of dust accumulation by gas dust thermal interaction. To this aim we consider a gas dust two component fluid. We carry out one dimensional numerical calculation which includes both momentum and energy interaction between the gas and dust.

In our model, the gas loses energy via thermal collision with the dust due to the gas dust temperature difference. The dust gains energy from the gas and emits energy to outside of the system by radiation. Only the dust absorbs radiation from surrounding radiation field. The dust receives gas drag force and the gas receives back reaction. Only the gas feels self pressure gradient.

As initial condition we assume that there is a dust density maximum in the gas. We add dust density profile with Gaussian form on uniformly distributed dust density. The gas density is constant. The dust to gas mass ratio is unity at the maximum of the dust density, and one percent at far from the dust density maximum. We adopt typical gas and dust temperature, which are plausible after dust heating by gas shock waves. The gas temperature is higher than the dust temperature. The gas and dust velocity is assumed to be zero at first. From this initial setting we evaluate time evolution of the system.

We find that the gas in high dust density region cools faster than the gas in low dust density region. This difference of the cooling time scale of the gas makes pressure gradient of the gas. The gas begins to flow into the low gas pressure region and the gas density increases in the region. Drag force induces the dust inflow and the dust density also increases there. Gas and dust density enhancement lasts until the minimum gas temperature attains the temperature of the surrounding radiation field and decreasing of minimum gas temperature stops. In our setting, we show that the maximum gas and dust density increase is around five times larger than the initial density.

The gas density increases as to the system becomes isobaric. Isobaric condition shows that the gas density enhancement is several times larger than the initial gas density. Drag force can enhance the dust density as the same order of the gas density increase.

Future work is to investigate the consequence of this dust density enhancement.

Keywords: protoplanetary disks, chondrule, shock wave heating, dust accumulation, thermal instability

Radial Accumulation of Dust Boulders at a Boundary between Super/Sub-Keplerian Flow in a Protoplanetary Disk

Tetsuo Taki^{1*}, FUJIMOTO, Masaki², IDA, Shigeru¹

¹Tokyo Institute of Technology, ²JAXA

In the process of planetesimal formation, spiral-in of dust particles toward the host star is the most serious difficulty. One of the mechanisms to halt the spiral-in is a radial pressure bump in the disk, at which the boundary between local super/sub-Keplerian flow exists. However, according to accumulation of dust particles at the super/sub-Keplerian transition point, the dust frictional force alters the gas density profile (e.g., Kato et al., 2012).

We think that accumulation processes of the dust particles at the pressure bump, which has the similar size with the bump presented by Kato et al. (2009, 2010). We have investigated the time evolution of dust density distributions due to drag force from the protoplanetary disk gas, taking into account backreaction from the

dust particles to the gas consistently with local 1-D and 2-D hybrid simulations. We treat the disk gas as a grid-hydrodynamics and the dust particles as super-particles.

In 1-D simulations, we found that the gas density distribution is seriously deformed as the dust accumulates at pressure bump in the case with backreaction. At once, the dust density distribution is radially expanded around the boundary between super/sub-Keplerian flow. Finally, the dust particles resume the inward drifts,

and their density distribution achieves the gradual peak in the radial direction. Then the maximum dust-to-gas density ratio is unity.

In 2-D simulations, we confirm the driving of streaming instability in the dust dense region formed by the radial pressure bump. Due to the effect of streaming instability turbulence, the maximum dust-to-gas density ratio raises to 5, which is larger than 1-D results. However it is lower than the result of the 2-D or 3-D MHD simulations presented by Kato et al. (2012), which include the effect of inhomogeneous MRI turbulence.

These dust-to-gas density ratios is too small to drive the gravitational instability, which forms the planetesimals quickly, and the pressure bump is not able to maintain the halting of the dust particles. Therefore, we conclude that the halting mechanism of pressure bump is not able to form the planetesimals very well by itself. Then we suggest the possibility that the effect of the maintenance or restoration to the pressure bump might increase the dust density and form the planetesimals via gravitational instability.

Keywords: planetesimal formation, protoplanetary disk

Dynamics of charged dust particles in the magnetic field related to the dust infall problem in protoplanetary disks

Kenichiro Hirai^{1*}, Yuto Katoh¹, Naoki Terada¹

¹Department of Geophysics, Graduate School of Science, Tohoku University

In Protoplanetary disks, the velocity difference occurs between the rotational speed of gas and dust particles due to the pressure gradient of the disk gas. Since the motion of dust particles is affected by the headwind of gas, dust particles lose angular momentum and eventually fall into a central star. However, since in the region close to the central star we can expect a finite magnitude of the intrinsic magnetic field and a high ionization rate due to the strong radiation from the central star, the effect of Lorentz force possibly plays important role in the dynamics of charged dust particles. For the discussion of the effect of Lorentz force in the dust infall problem, we quantitatively evaluate the effect of background magnetic field to the charged dust particle.

By assuming minimum mass solar nebula model and constant plasma beta throughout the disk, we estimate the gyroperiod of charged dust particles. We also assumed the charge state of dust particles by referring the observation result of charged particles in the Saturnian E-ring by Cassini spacecraft [e.g., Horanyi et al., 2004]. For the case that the gyro period approximately equals to the stopping timescale by headwind (e.g., Weidenschilling, 1977) of gas at 1 AU, dust particles with the radius of 1 cm should be charged $\sim 10^{17}$ e (e: elementary charge).

The charge state of dust particles with the radius of 1 μ m measured in the Saturnian E-ring has been reported to 1000 e (e.g., Horanyi, 2004). Assuming that these dust particles collide and coalesce each other and become 1cm sized dust and that the charge state is proportional to its volume, we obtain 10^{15} e for 1 cm dust particles. In the present study, we study the relation between the radius and charge state of dust particles and the validity of the model assumed in the present study for protoplanetary disks so as to discuss electromagnetic effect to the dust particle quantitatively.

Keywords: protoplanetary disk, dusty plasma

Tidal orbital evolution of retrograde hot jupiters

Naoya Okazawa¹, Kiyoshi Kuramoto^{1*}

¹Hokkaido University

Recently, retrograde hot jupiters with orbits run counter to the spin of their central stars have been discovered. For such a hot Jupiter with large orbital inclination, it is hard to think that the planet formed in-situ on a proto-planetary disk or, that it moved to the present position by the interaction with disk gas after planet formation, because the planetary orbit is kept almost align with the disk plane in these processes. Then, the "slingshot scenario" have been proposed as a likely formation scenario of these planets. In this scenario, a gas giant planet with highly elliptical orbit with large inclination has once formed by gravity scattering among gas giant planets formed in a proto-planetary disk. And then, the tidal action of its central star induces the orbital evolution to hot Jupiter.

There remain questions, however, in the processes of such tidal action. For example, tidal action is modelled by assuming dynamical tide in some previous works, because the orbital evolution begins from a highly elliptical orbit (e.g. Nagasawa et al. 2008). However, as the eccentricity becomes small with orbital evolution, it would become appropriate to consider equilibrium tide. In addition, the strength of tidal friction has still been poorly constrained.

This study presents our theoretical analysis of the tidal orbital evolution of six hot Jupiter whose primary stars' ages are known and attempts to estimate likely processes of tidal action and the intensity of tidal friction.

In the tidal interaction, the vector sum of angular momentums of planetary orbit, stellar rotation and, planetary rotation is preserved. Moreover, the angular momentum of planetary rotation is too small to affect the evolutionary pathway. Since the orbital angular momentum of a retrograde planet is always conveyed to that of stellar rotation, the past orbit should have larger angular momentum than the present. That is, the evolutionary pathway kept the current orbital angular momentum has the smallest pericenter distances. For each of the six planets, the time constants of the pericenter passage during such preserving evolutionary pathway are longer than that of planetary free oscillation. This shows that an equilibrium tide model is appropriate for these planets.

By using the equilibrium tide model(Eggleton 1998), numerical calculations of orbital evolution backward in time for the age of each planetary system is performed. Since the tidal dissipation constant which specifies the strength of tidal friction has large uncertainty, it is taken as a parameter. Its value which may reproduce the orbital evolution from an extended elliptical orbit to the present orbit is obtained exploratory.

For each planet, there exists solutions whose early orbit meets the conditions expected from a slingshot scenario (An semi-major axis before the age of a system is 2-3 AU. It does not collide with a central star on the way of orbital evolution). The dissipation constant that agrees with the above conditions can be constrained in a narrow range for each planet. It appears that there is a correlation between planet radius and dissipation constant. The dissipation constant of Jupiter derived from the orbital dynamics of Jovian satellites also follows this correlation.

Using acquired value of dissipation constant, the past tidal heating rate is also estimated. The six retrograde planets may have received tidal heating 0.05-2 times as strong as central star radiation for the earliest billions of years. Furthermore, the orbits of these planets are maintained over the next billions of years or more without falling to the central stars. This would be conformable with the fact that many hot Jupiters exist.

On the magnetic activities in hot Jupiters

Yuki Tanaka^{1*}, SUZUKI, Takeru K.¹, INUTSUKA, Shu-ichiro¹

¹Department of Physics, Nagoya University

Recently theoretical studies on thermal evolution of hot jupiters invoked Ohmic dissipation to account for extraordinary large radii of some objects.

Those analyses suggest the existence of significantly strong magnetic fields in hot jupiters.

To test this hypothesis it is important to investigate possible consequence of magnetic fields in gaseous giant planets.

Since gaseous giant planets are supposed to have large convection zones, magnetic field mediates energy transfer from the interior to the exterior of the atmosphere.

In this talk we develop a model of magnetically driven wind from a gaseous planet and investigate the resultant mass loss.

This work may provide a possible consistency check of theories with observations of hot jupiters.

Keywords: exoplanet, mass loss

Capture and orbital evolution of irregular satellites by gas drag from circumplanetary disk

Ryo Suetsugu^{1*}, Tetsuya Fujita¹, Keiji Ohtsuki¹

¹Dept. Earth Planet. Sci., Kobe Univ.

Many satellites are orbiting about the giant planets in the Solar System. The number of known satellites has been increasing significantly due to advancement of observation technology, and studies of these small bodies help us understand better not only their origin but also formation processes of giant planets. Satellites are classified into regular satellites and irregular satellites. It is thought that regular satellites formed in circumplanetary disks around giant planets, because their orbits are nearly circular and coplanar. On the other hand, orbits of irregular satellites are highly eccentric and inclined, thus, they are thought to be planetesimals captured by the planets through some energy dissipation.

Although several energy dissipation mechanisms for capturing irregular satellites have been proposed by previous works, most of them seem to have difficulty in explaining capture of the irregular satellites of Jupiter. However, Cuk & Burns (2004) argued that a cluster of prograde irregular satellites of Jupiter may be collisional fragments of a single planetesimal captured by gas drag from the circumjovian disk at the final stage of the formation of Jupiter. They integrated orbits of this parent body backward in time, and found that the parent body experienced a period of temporary capture by Jupiter before it became gravitationally bound by Jupiter. If the gas density of the circumjovian disk was too high, a captured planetesimal would likely spiral into Jupiter rather quickly due to large energy dissipation, but its lifetime within the disk is expected to be longer if a gap in the solar nebula was formed by the gravity of Jupiter and the gas density in the circumjovian disk was lower. Therefore, if planetesimals with low energy are temporarily captured by Jupiter for an extended period of time near the end of Jupiter's formation, they may survive for a long time and even weak energy dissipation may be sufficient for capturing them as irregular satellites or their progenitors. However, temporary capture itself has not been examined in detail. Recently we investigated temporary capture of planetesimals by a planet using three-body orbital integration. As a result, we found that temporary capture orbits could be classified into four types and evaluated the rates of temporary capture (Suetsugu et al. 2011 AJ 142, 200; Suetsugu & Ohtsuki, MNRAS, in press).

Growing giant planets can capture planetesimals by gas drag from circumplanetary disk (Fujita et al, submitted to AJ). In order to reveal origin of irregular satellites, it is also important to examine orbital evolution after the capture. In the present work, we will discuss capture and orbital evolution of irregular satellites due to gas drag from circumplanetary disk.

Keywords: planet, satellite